We have 2 lectures left:

Feb. 16th – lecture 12 – Today's and Feb. 21st
Feb. 23th – lecture 13 – and Feb. 28th

Mar. 2nd – exam at CAMK at room 18/19
Mar. 9th – overview of exam, signing cards

You can still upload your HW#6 and hands-on results
Up to the Feb. 19th (Copernicus birthday).

Overview of this HW#6 will be on Feb. 23rd

Summary after 10th and 11th lecture:

10th lecture:

Accreting physics:

- accretion disc
- accretion efficiency
- Eddington luminosity
- flux from accretion disc
- inner disc temperature

X-ray binaries:

- HMXB, LMXB
- transients
- eclipsing X-ray binaries
- X-ray binary pulsars
- X-ray bursters
- QPO sources

Accreting black holes:

- spectral state transition
- X-ray reflection from accretion disc
- Comptonization in hot corona
- disc truncation
- iron K alpha line
- ULX sources

11th lecture:

SNRs:

- shock heated plasma
- images in different line's emission
- kinematics and shock evolution
- emission from SNe

ISM in X-rays:

- extinction on heavy ions
- distribution over galactic plane

Galactic Center:

- Sgr A* radio source
- mini-spirals in radio emission
- morphology around GC
- hot bubble of ionized gas emission
- flares from GC
- iron line emission as a trace of past activity
- surface brightness
- two-phase medium

The theory of different emission processes across astrophysical objects:

- Solar system objects
- Nuclear Burning Stars
- White Dwarfs
- Cataclysmic Variables
- Classical Novae
- Pulsars and Isolated Neutron Stars
- Accreting Neutrons Stars and Black Hole binaries
- Supernova Remnants
- Interstellar Medium
- Galactic Center

- Nearby Galaxies
- Active Galactic Nuclei
- Clusters of Galaxies
- Gamma - Ray Bursts
- Cosmic X-ray Background

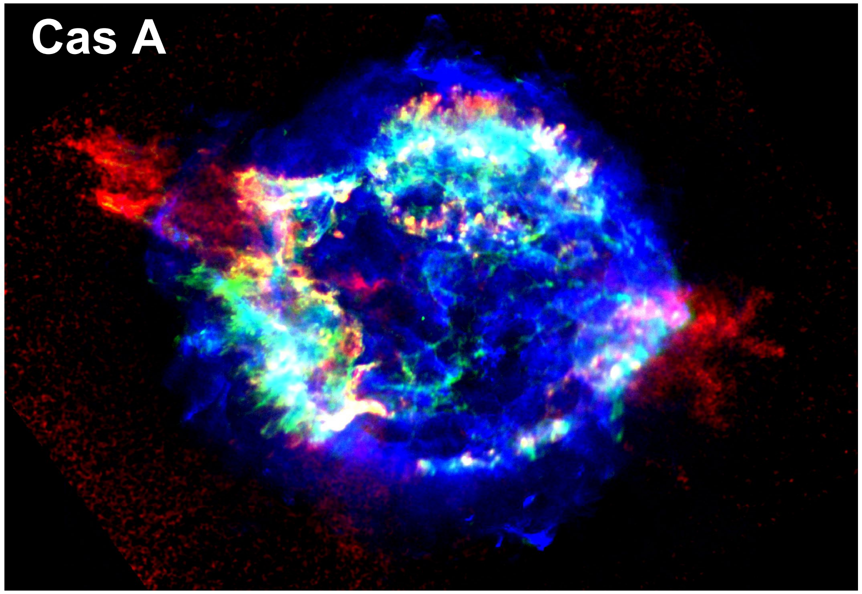

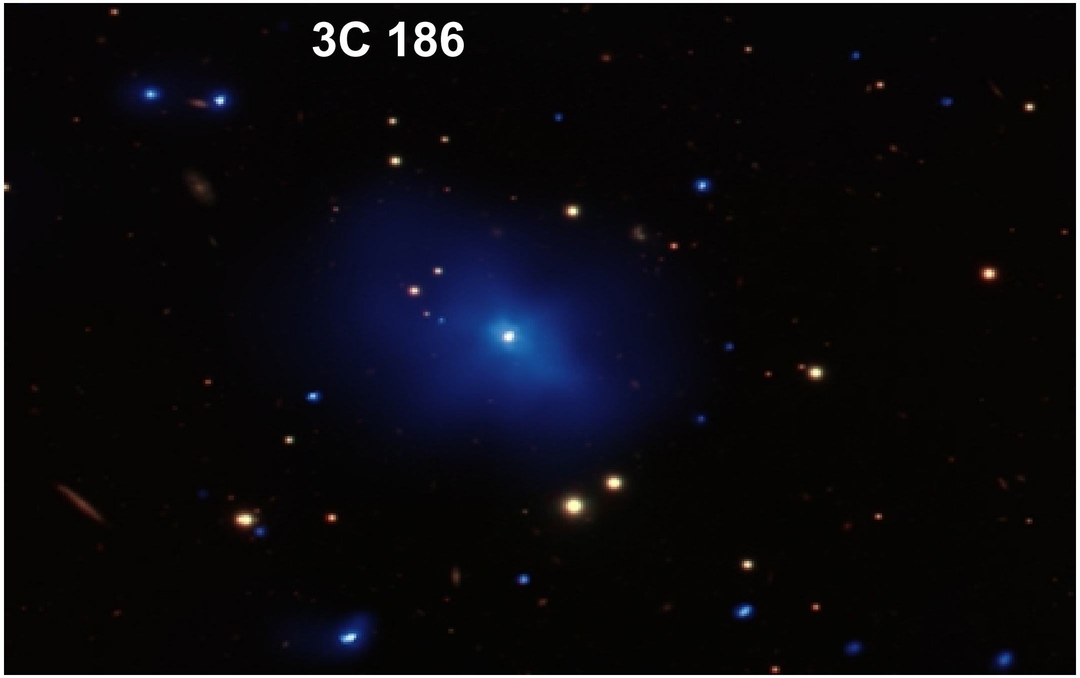

Lecture 12th : Everything beside AGN:

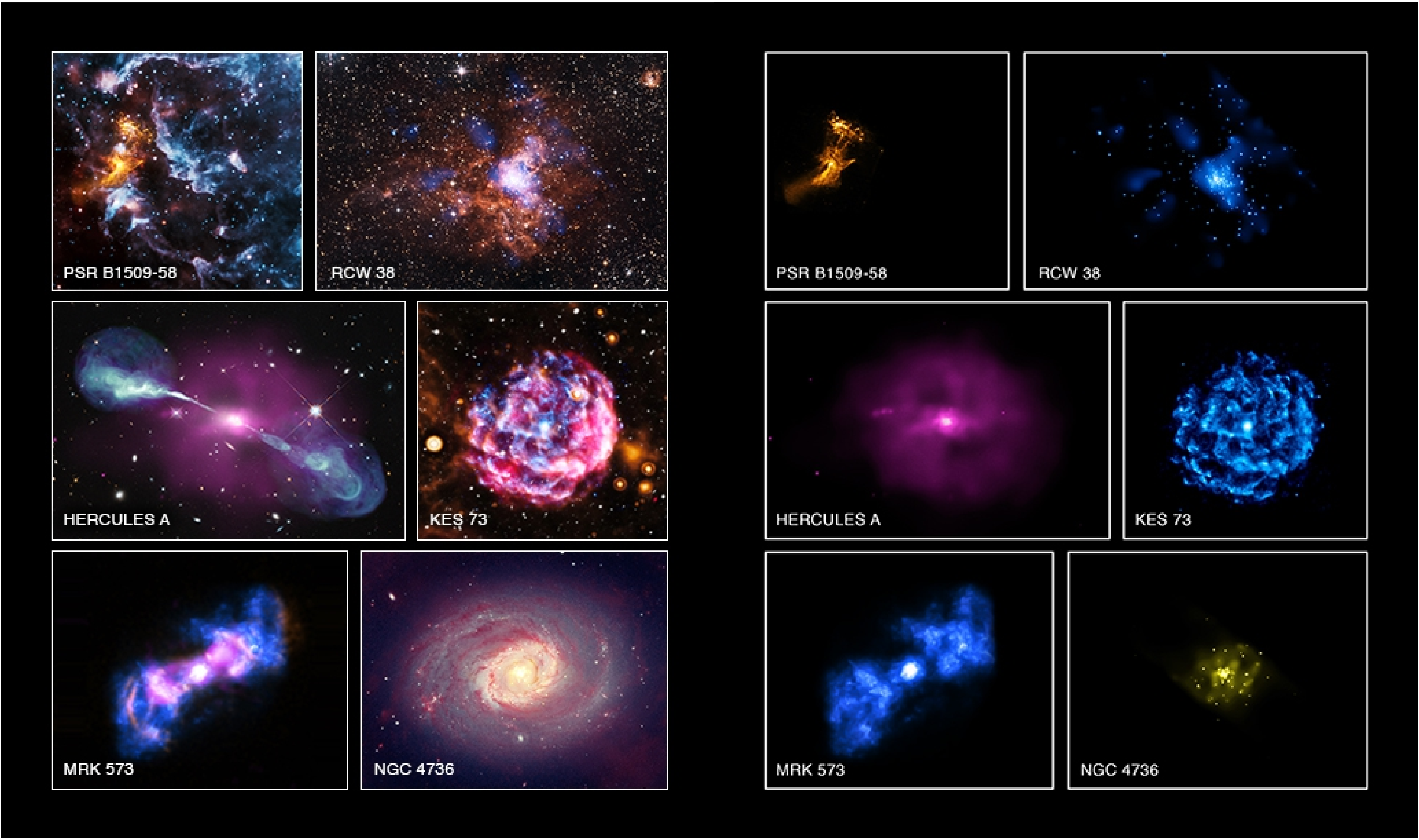

Chandra image collection

Inter-stellar Medium – strong absorption:

ISM – the space between the stars in not empty …
- – interstellar extinction discovered by Trumpler 1930.
- – cold neutral Hydrogen, ward ionized gas HII regions.

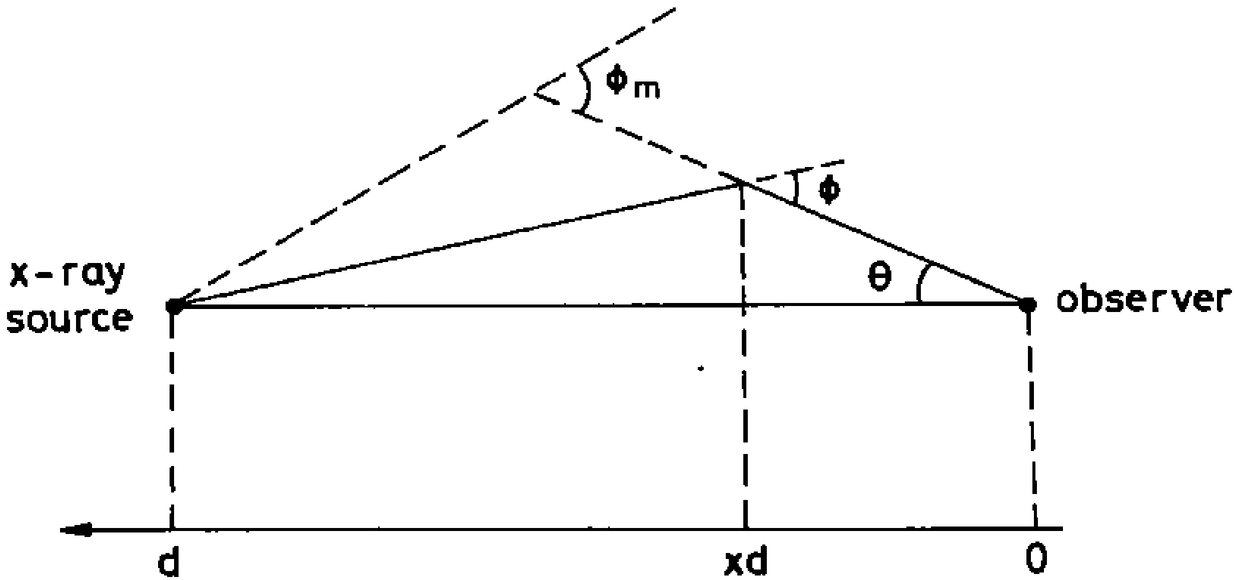

Fig. 1. Illustration of geometries

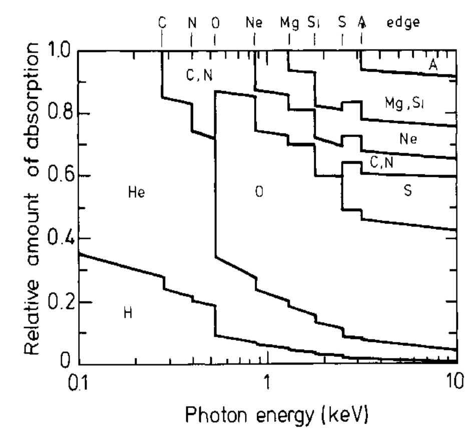

Fig. 2. Relative importance of different elements in the interstellar medium for the absorption of soft X-rays (Seward 1975)

HIM – hot interstellar medium first in X-rays Giacconi+ 1962, and soft component (< 2 keV) Bowyer + 1968.

ISM – Soft X-ray emission of gas:

Observations of OVI line towards the different stars Jenkins+ 1974 UV Copernicus spectrometer. Using the ratio of:

$$N(S_{IV})/N(O_{VI})$$

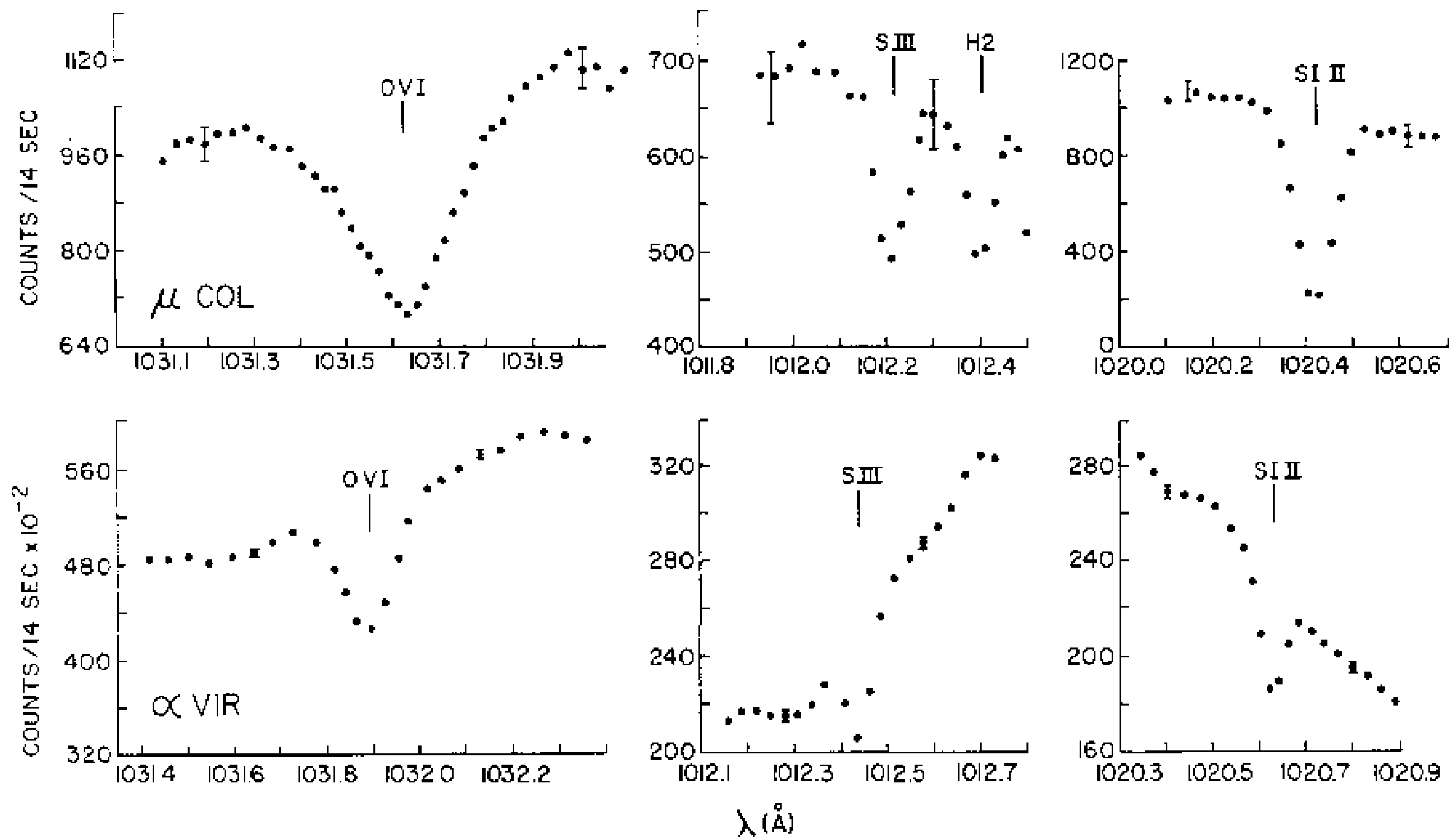

They have estimated HIM temperatrue as:

$$2\times10^{5}\,K < T < 2\times10^{6}\,K$$

ISM – Soft X-ray emission of gas:

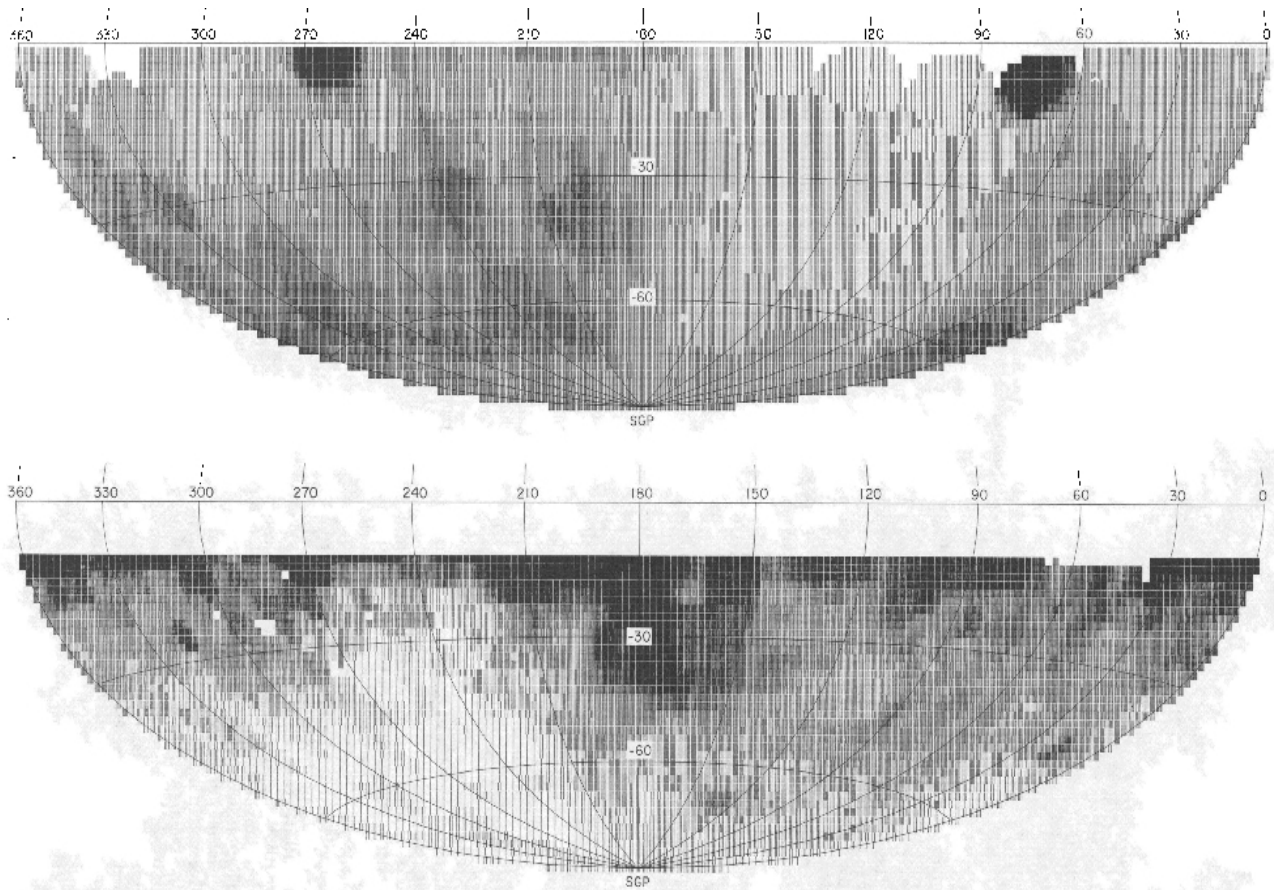

Fig. 1a.—C-band intensity map of the southern galactic hemisphere. The darkness of the shading is proportional to X-ray intensity. Two extremely intense features near the galactic plane at longitudes $\sim 70°$ and $\sim 260°$ are created by the Cygnus Loop and Vela supernova remnants.

Fig. 1b.—Map of the neutral hydrogen column density data compiled by Daltabuit and Meyer (1972). Each line of shading per resolution element corresponds to 10^{20} H atoms cm^{-2}. Blanks indicate no data.

0.13- 0.28 KeV
C – band soft X-ray emission of the southern galactic hemisphere Cygnus loop and Vela SNRs are present.

Neutral hydrogen column density maps.

Soft X-ray emission decreases with increasing neutral H column density. Bulk of the cool gas is beyond the X-ray emitting region. Sanders + 1977.

ISM – Soft X-ray emission of gas:

Local Hot Bubble model
Sanders + 1977.
Solar System is surrounded by a bubble, filled with hot plasma of:

$$T \sim 10^6\, K$$
$$n \sim 5 \times 10^{-3}\, cm^{-3}$$

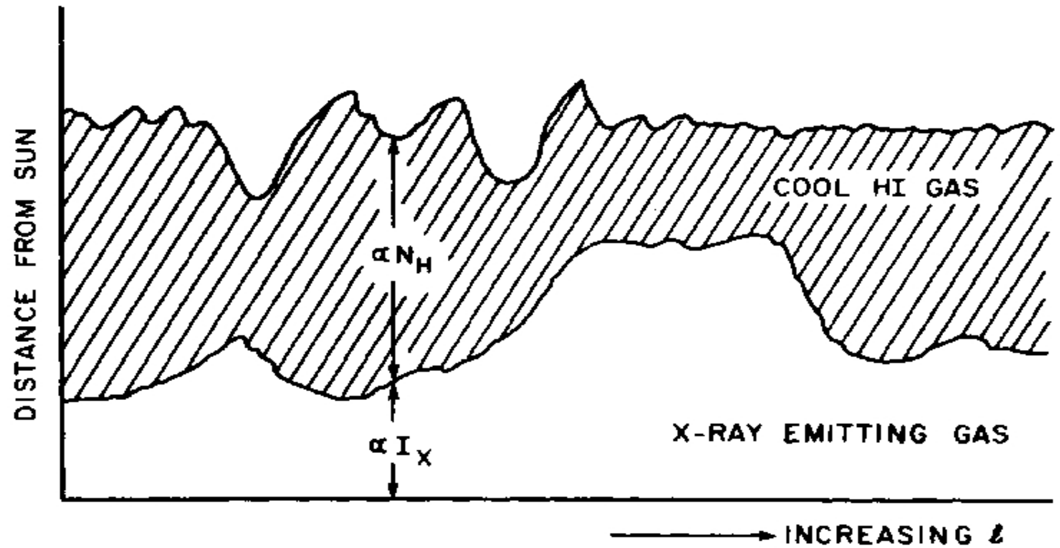

FIG. 3.—Schematic picture of the hypothesized distribution of X-ray emitting gas and neutral hydrogen (distance from the Sun as a function of galactic longitude) at an arbitrary intermediate galactic latitude. At a different galactic latitude a quantitatively different but qualitatively similar distribution would result.

displacing HI.

Frisch + 1983 – Sun is in the local HI void with column density down to:

$$N_H \sim 10^{18}\, cm^{-2}$$

ISM – extinction:

Extinction is due to both absorption and scattering by gas and dust.
Optical extinction arises primarily from scattering off grains of dust.

X-ray extinction is primarily due to absorption (wabs model) but also dust is important. X-ray source behind dense dust cloud is expected to be surrounded by halo of faint and diffuse X-ray emission.

With one single measurement in X-rays one can determine:

- from X-ray cutoff the total extinction due to photoelecric absorption,
- total scattering from the surrounding diffuse X-ray halo.

Lunnar occultation of Sco X-1

ISM – connection of visual extinction vs N_H:

Source	N_H (Lit)	N_H (pwl)	err	χ^2	N_H (thb)	err	χ^2	N_H (bbd)	err	χ^2
Cyg X-1		4.1	0.4	1.0	4.0	5.9	1.0	2.6	0.3	1.1
Cyg X-2	3[1]	2.5	0.2	1.9	2.5	0.2	2.1	0.7	0.1	2.7
Cyg X-3		33.1		1.7	40.5		1.7	0	24.	5.4
Ser X-1		5.1	0.5	1.2	5.0	9.0	1.2	3.0	0.3	1.2
GX 17+2	19[1], 21[2]	20.6	3.3	1.2	23.4	17.	1.5	17.9	1.2	1.3
GX 13−1	29[1]	27.9	66.	1.1	31.7	33.	1.0	0	28.	3.2
GX 9+9	2[1]	2.6	0.3	1.5	2.5	3.0	1.5	0.8	0.2	1.5
GX 9+1	15[2], 18[1]	15.6	4.6	1.0	18.7	57.	1.3	13.6	1.2	1.0
GX 5-1	33[1]	30.8	6.8	1.2	34.8	28.	1.5	27.8	2.2	1.1
GX 3+1	12[1], 16[2]	17.0	2.3	1.2	17.8	48.	1.2	14.2	0.9	1.2
BQ 1731-260		12.6	2.1	1.3	12.8	32.	1.3	10.0	1.9	1.3
GS 1734-275		11.6	1.4	1.2	10.8	4.4	1.2	8.3	0.2	1.2
GX 349+2	8[2]	9.6	0.7	1.8	37.8	2.5		7.1	0.5	1.7
4U 1820-30		2.4	0.4	1.2	2.1	0.5	1.2	3.6	0.2	1.2
4U 1755-338		3.8	0.2	1.1	3.7	1.6	1.0	1.8	0.1	1.5
4U 1705-44		14.7	1.8	1.2	16.3	34.	1.4	12.3	0.7	1.2
GX 339-4		6.7	0.3	1.5	5.9	0.6	1.5	3.8	0.1	1.5
V801 Ara		3.6	0.5	1.0	3.5	2.7	1.0	0.3	1.1	1.1
4U 1556-60		3.2	1.4	1.3	3.2	2.1	1.4	1.5	0.9	1.3
Cir X-1		22.3	6.5	1.6	24.1	38.4	2.6	19.9	2.7	1.6
LMC X-1		9.4	0.8	1.1	16.0	1.0	3.5	5.9	0.5	1.1
LMC X-2		1.1	0.5	1.1	0.9	0.3	1.1	0.0	0.3	1.3
LMC X-3		1.1	0.4	1.0	0.7	0.1	1.0	0.0	0.3	1.5
4U 1543-47		4.9	0.1	1.0						
PKS 2155-304		0.2	0.0	1.8						
Cas A		18.3	0.37	1.35						
Tycho	4.0									
Kepler	6.0									
Crab		2.9	0.1	2.8	2.06	0.1	3.0	3.4	0.05	4.6

Peterson + 1995

ISM – connection of visual extinction vs N_H:

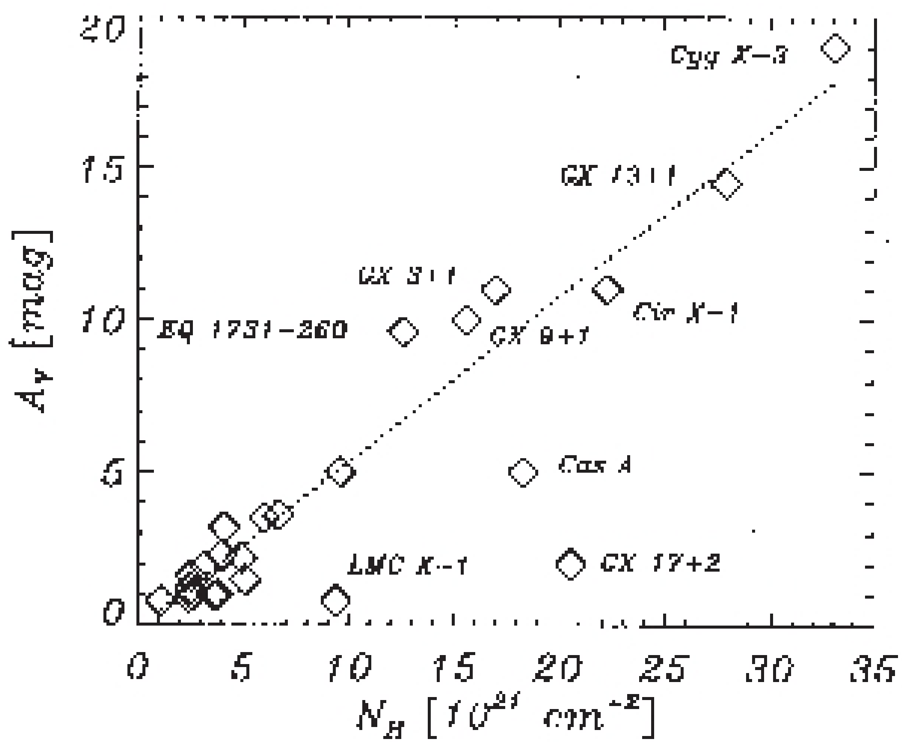

Fig. 3. Visual extinction vs. equivalent hydrogen column density. The fit (dotted line) does not contain GX 17+2 and LMC X-1. It yields N_H = 1.79   0.03 A_V [mag] × 10^{21}[cm ^{2}]

Peterson + 1995

$$A_V = 0.56\, N_H [10^{21}\, cm^{-2}] + 0.23$$

ISM – in X-rays:

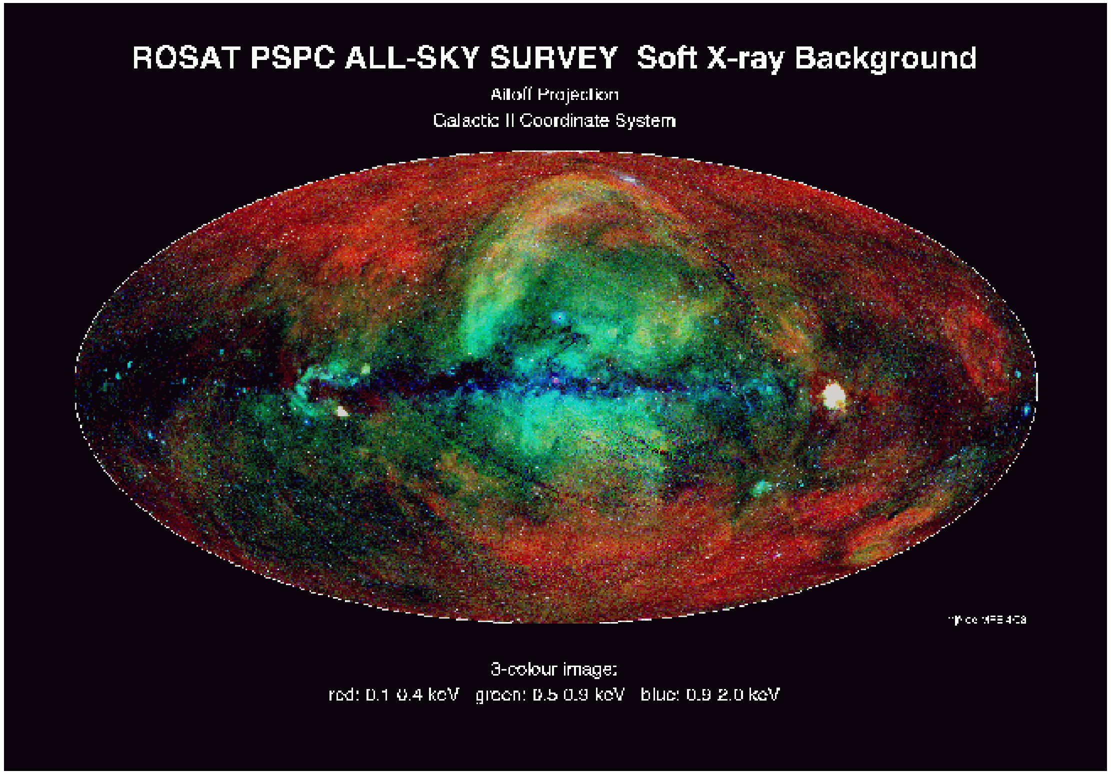

All -Sky Survey:

1) unresolved Galactic point sources,

2) unresolved extragalactic point sources (80% of total emission),

3) diffuse *local* emission (Local Bubble),

4) diffuse *distant Galactic* emission (hot ISM and Galactic Halo),

5) diffuse warm-hot intergalactic medium (WHIM)

6) local emission due to CT of solar wind with geocorona.

X-rays from nearby galaxies:

ROSAT – wide field of view, better angular resolution allowed to study Super Soft Sources (SSS) and ISM from other galaxies.
Chandra and XMM-Newton the deepest look at galaxies in X-rays.

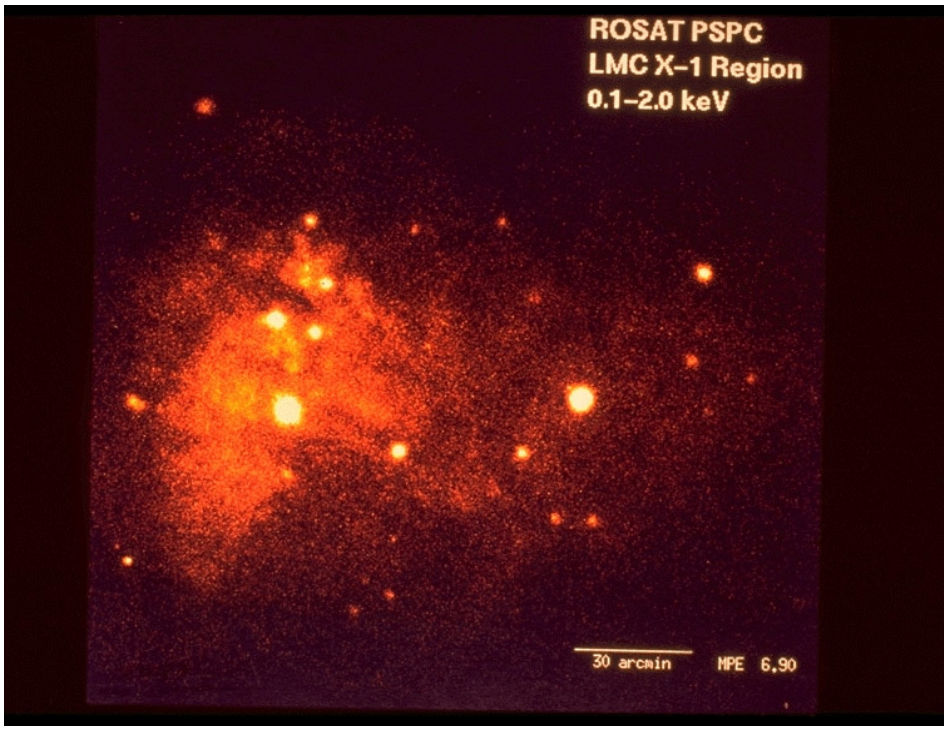

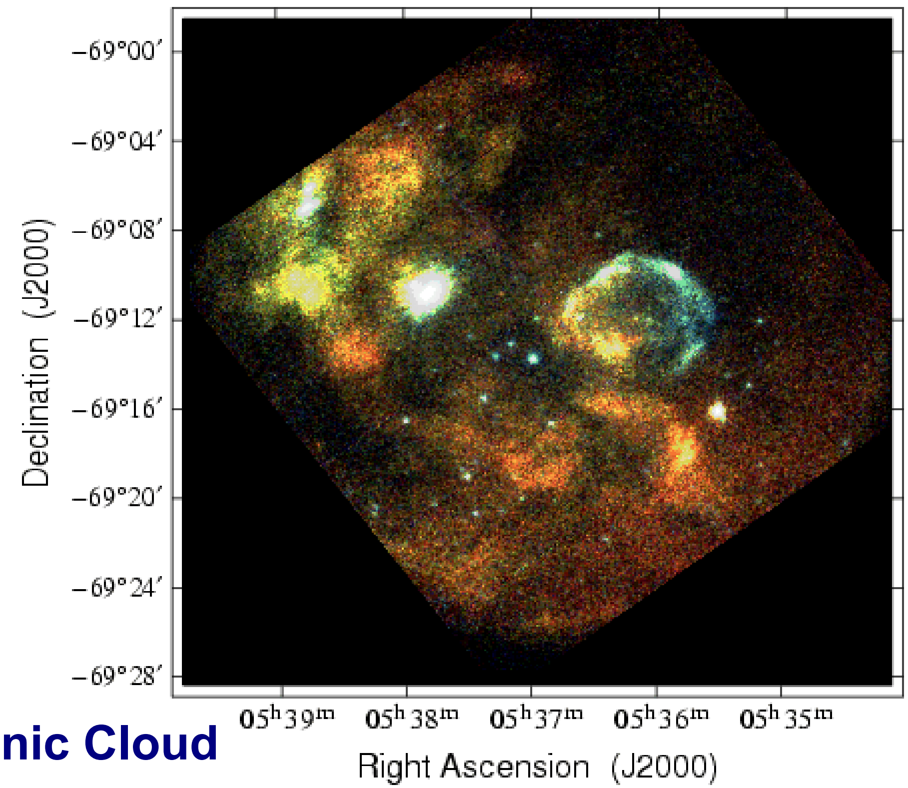

Large Magellanic Cloud

Right – XMM-Newton image is a zoom-in by a factor of six compared to the ROSAT image.

X-rays from nearby galaxies:

X-rays from nearby galaxies:

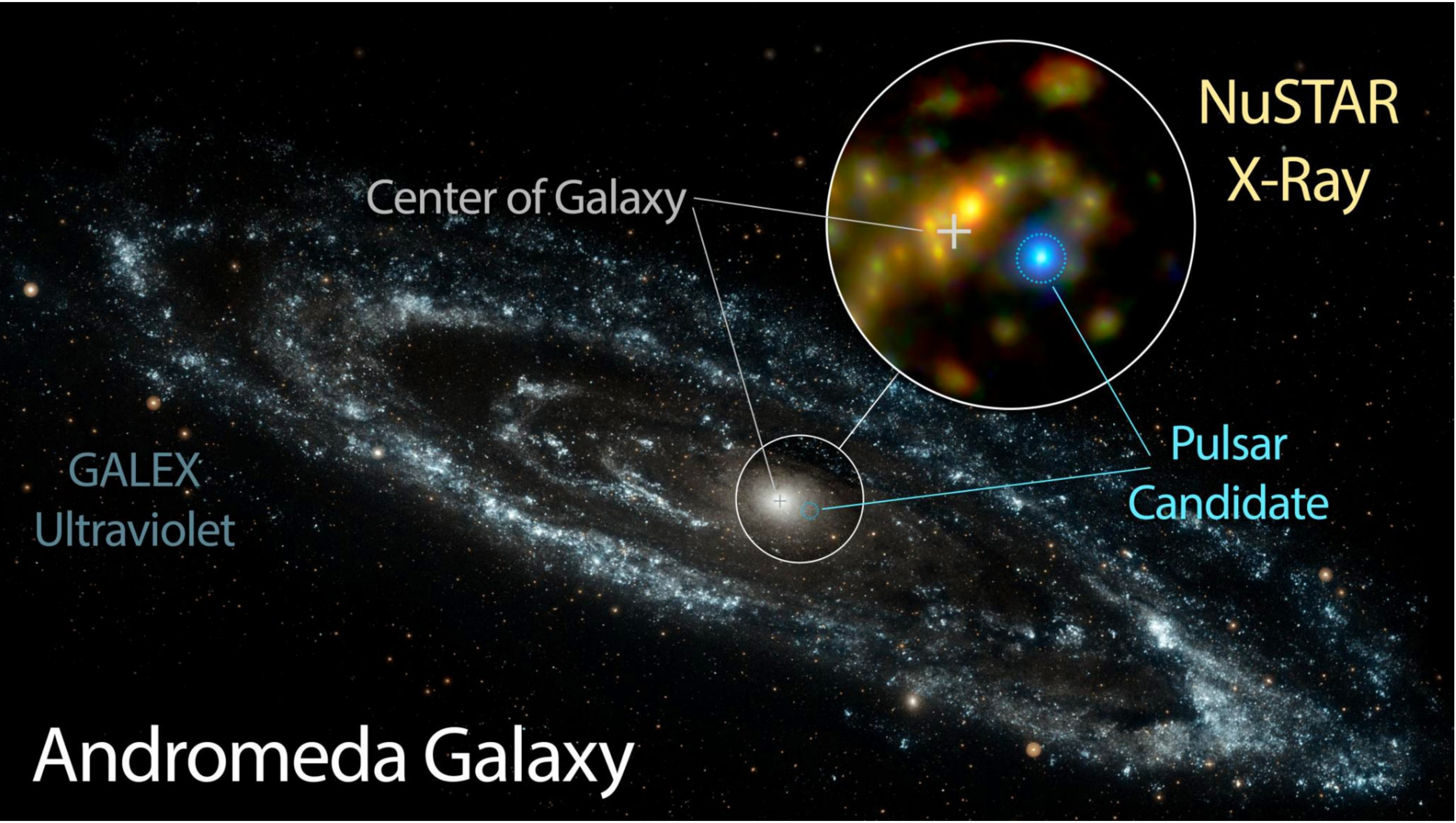

Point like emission components:

- X-ray binaries (XRBs)
- Supersoft sources (SSS)
- Supernovae (SN)
- Supernovae remnants (SNRs)
- Nuclear sources
- Ultra-luminous X-ray sources (ULXs)

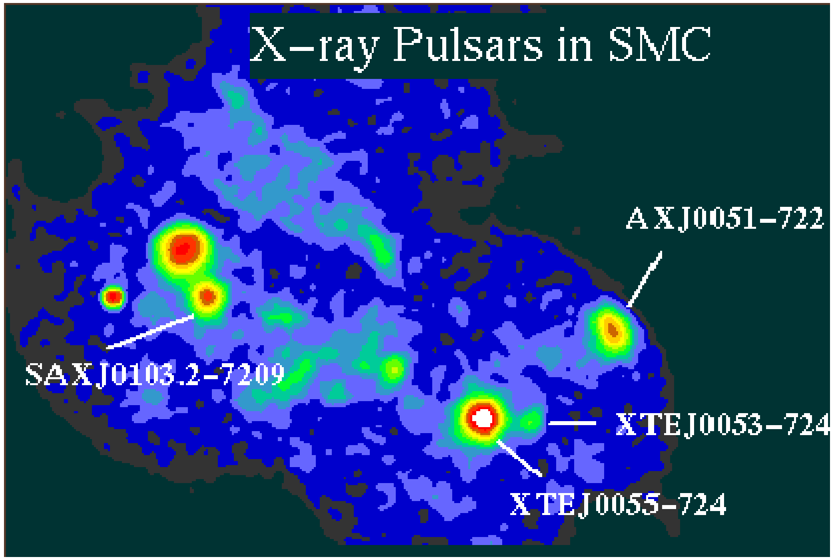

Often X-ray population of the target galaxy is confused by foreground stars in the Milky Way and background objects (galaxies, galaxy clusters, and AGN).

Classification can be based on:

- position and/or time variability with counterparts observed in other energy bands,
- X-ray time variability,
- hardness rations,
- energy spectra.

Point like emission components:

XRBs contribute the major fraction to the host galaxy's X-ray luminosity:

HMXBs – lifetime limited by the nuclear time scale of the massive donor star to less than $10^6 – 10^7$ yrs, comparable to the duration of star formation event.

LMXBs – lifetime limited also by binary orbit decay time-scale $10^9 – 10^{10}$ yrs comparable to the hst galaxy. The population of LMXBs is proportional to the total stellar mass of a galaxy.

Distribution of HMXRs and LMXBs in the Milky Way Grimm + 2002, RXTE ASM.

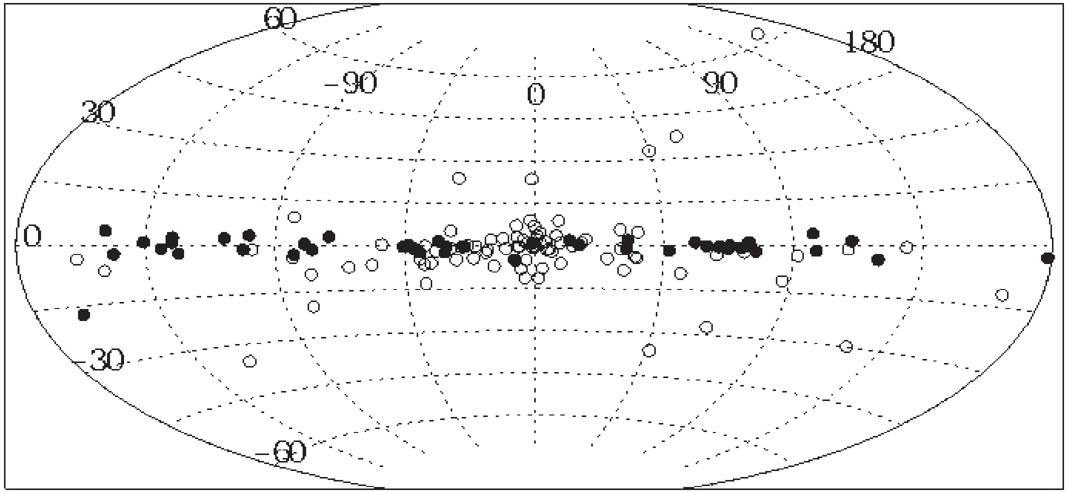

Fig. 1. Distribution of LMXBs (open circles) and HMXBs (filled circles) in the Galaxy. In total 86 LMXBs and 52 HMXBs are shown. Note the significant concentration of HMXBs towards the Galactic Plane and the clustering of LMXBs in the Galactic Bulge.

Point like emission components:

Log(N) – Log(S) distribution (number-flux relation):

$$N(>S) = k * \left(S^{(-a)} - S_{max}^{(-a)}\right) \qquad N(>S) = k * S^{(-a)}$$

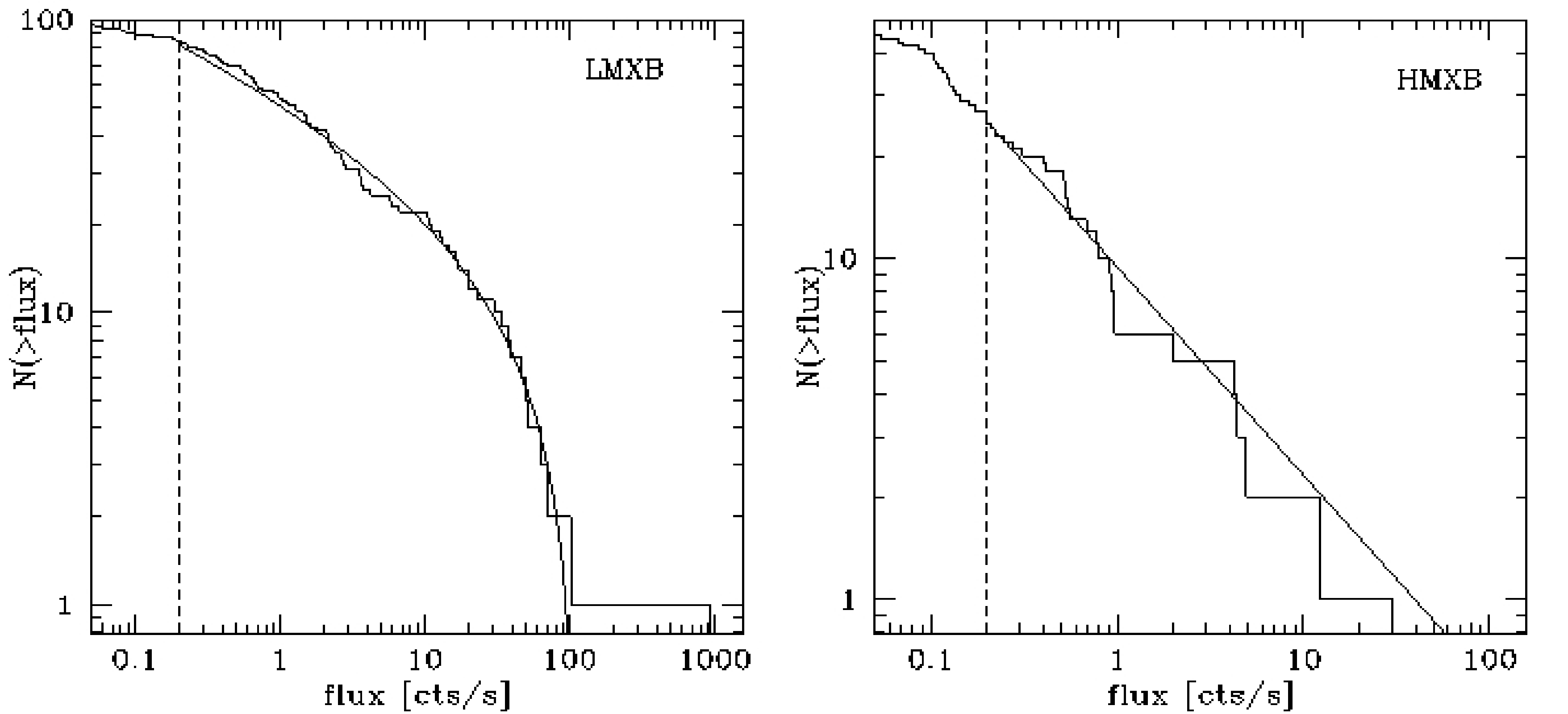

Fig. 5. Number-flux relation for galactic X-ray binaries. The vertical dashed line corresponds to our completeness limit of 0.2 cnts s^{-1}. The solid lines are the best fit models to the ASM data – a power law for HMXBs and a power law with cutoff in the differential Log(N)-Log(S) distributions at 110 cnts s^{-1} for LMXBs (see Eqs.(2) and (3)).

Point like emission components:

Luminosity function, dN/dL:

$$N(>S) = \int_{L_{min}}^{L_{max}} \frac{dN}{dL} \times \frac{M(<r)_{ASCA}}{M_{total}} \, dL$$

$$r = \sqrt{\frac{L}{4\pi S}}$$

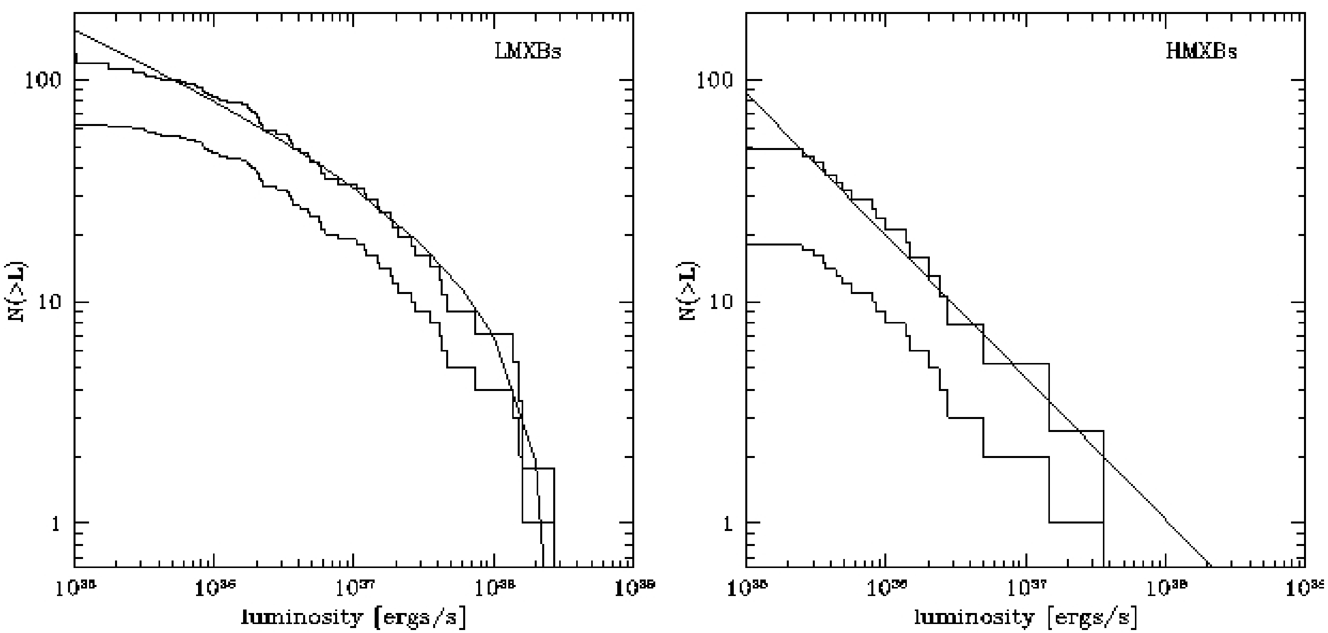

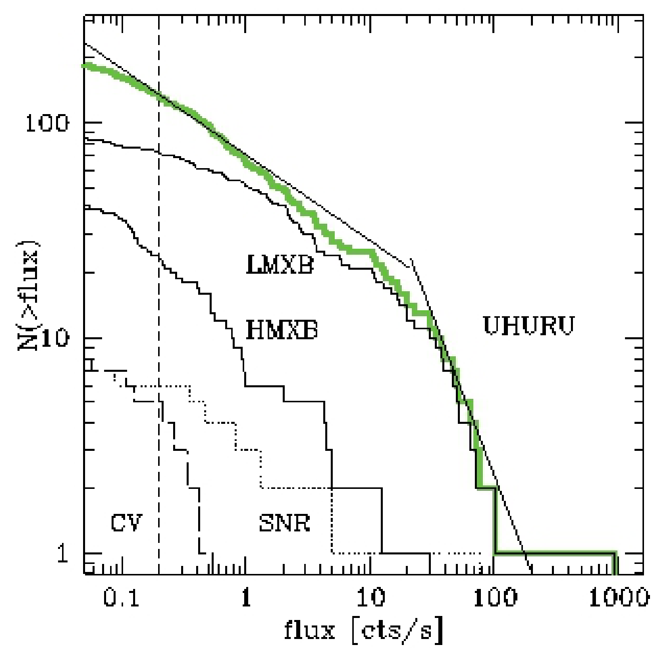

Fig. 12. The apparent (thin histogram) and volume corrected (thick histogram) cumulative luminosity function for LMXBs and HMXBs. The solid lines are the best fits to the data.

Point like emission components:

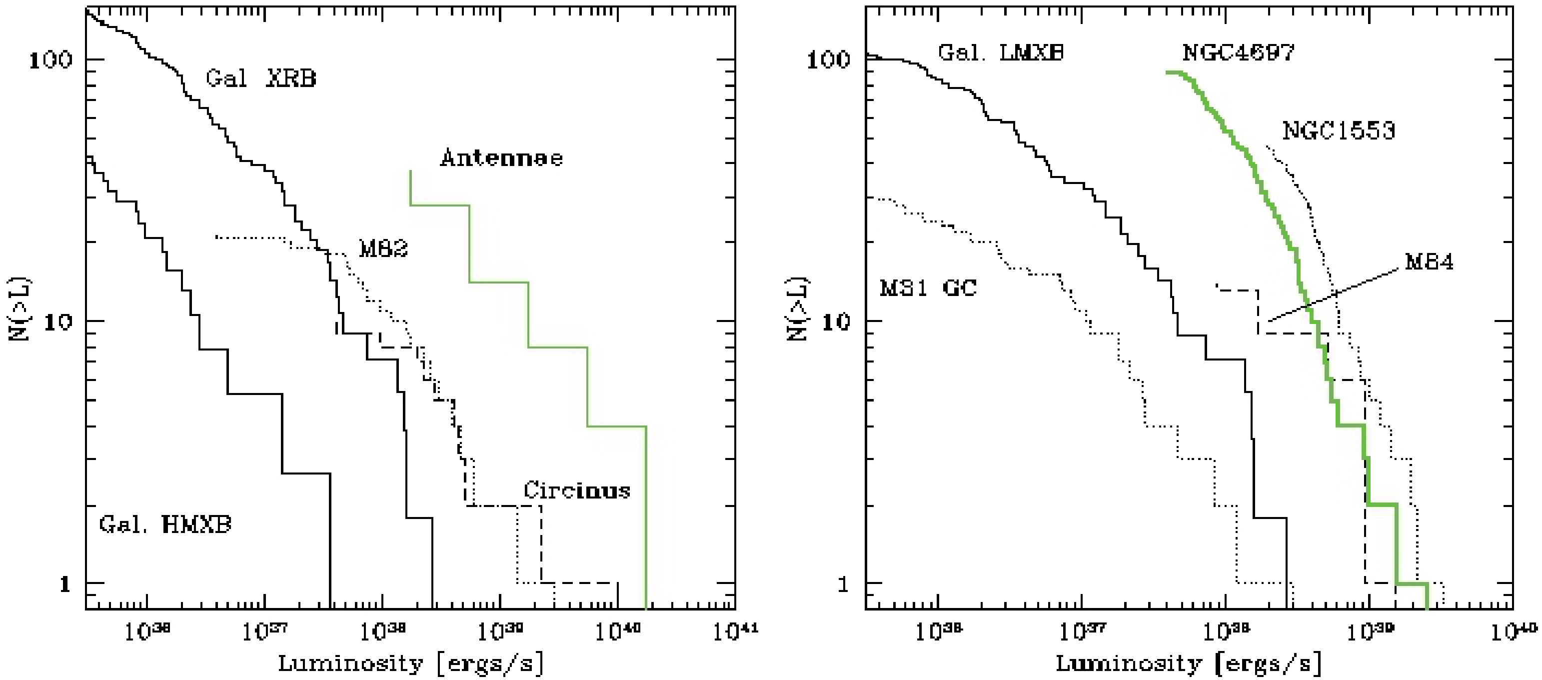

Fig. 16. Cumulative luminosity functions of galaxies observed with CHANDRA. The left panel shows actively star forming spiral galaxies that include NGC 4038/39 and M 82 which are supposed to be dominated by HMXBs. For comparison the luminosity functions of Galactic X-ray binaries and HMXBs alone are shown. The right panel shows elliptical galaxies including the SO galaxy NGC 1553. For comparison the luminosity function of Galactic LMXBs is shown.

Other galaxies in comparison with our Galaxy Grimm + 2002.

Point like emission components:

M 33 X-7 - the first eclipsing black hole
Pietsch, Mochejska + 2004
P=3.45 d
When i=90º
M= 2.1- 3.0 M_{Sun}.

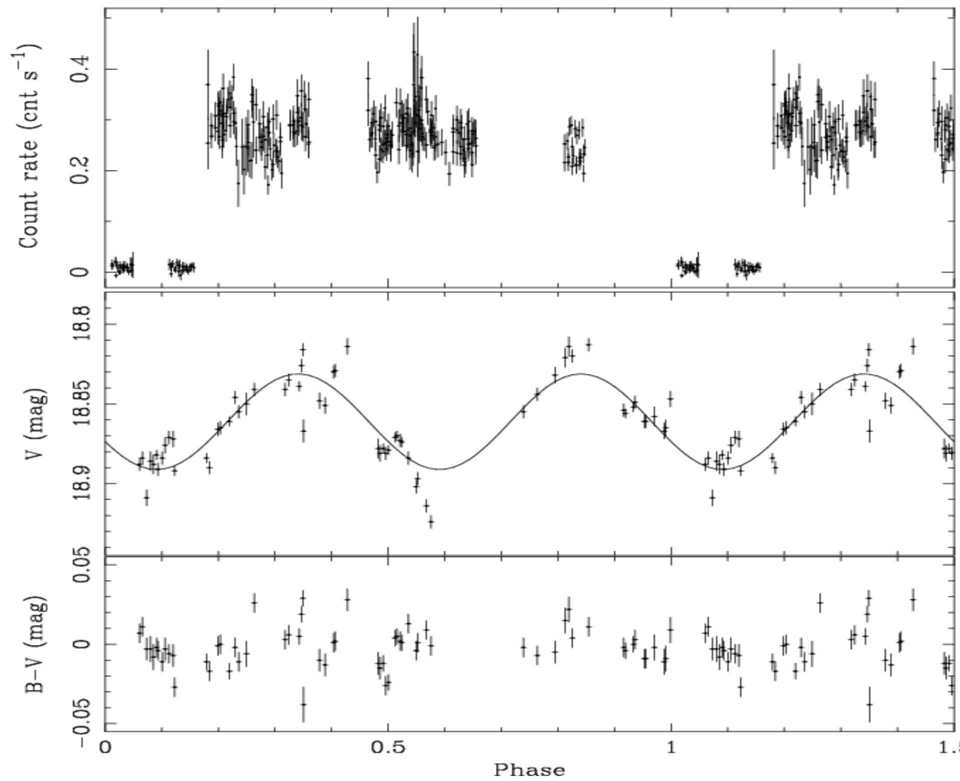

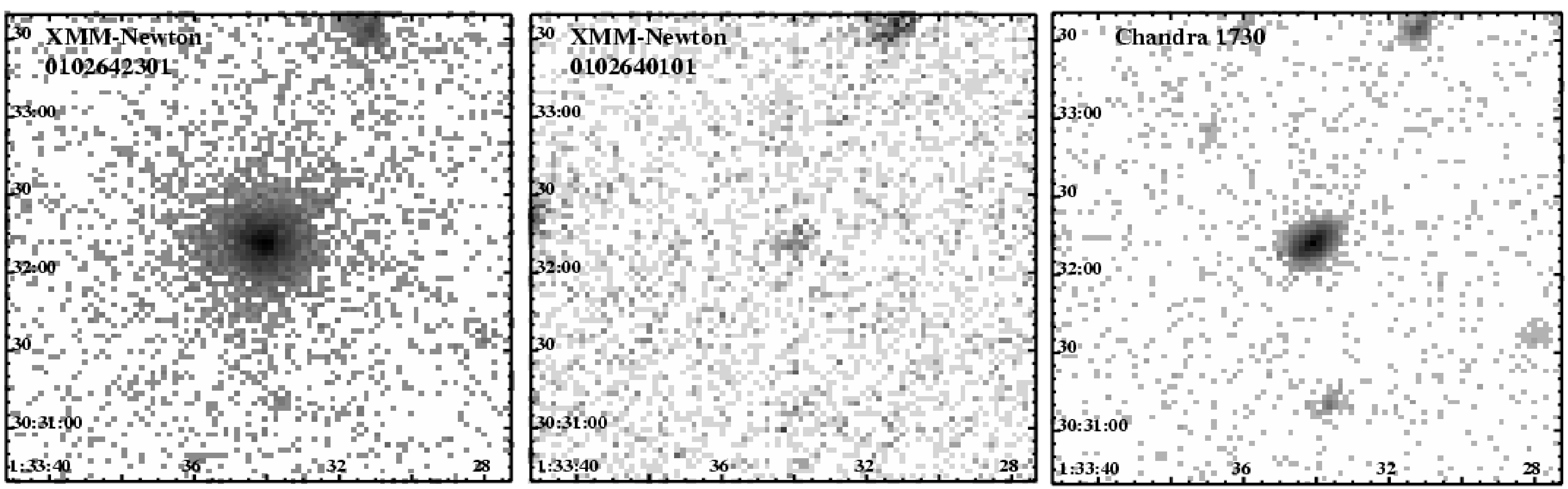

Ultra luminous X-ray sources (ULXs):

Point sources in nearby, normal galaxies, for which the inferred X-ray luminosity exceeds the Eddington limit for a 10 M№ black hole i.e. 1.3 x 10^{39} erg/s;

$$L < L_{Edd} = \frac{4\pi c G M m_H}{\sigma_T} = 10^{38} \frac{M}{M_{Sun}}$$

They may represent:

1) rare states or phases of accretion in binary systems
2) they may harbor intermediate black hole (IMBH)

$$T \propto M^{-1/4}$$

$$SMBH, \quad 10^{8-9} M_{Sun}, \quad T \approx 10^{4-5} K$$

$$IMBH, \quad 10^{2-5} M_{Sun}, \quad T \approx 10^{6-7} K$$

$$GBHB, \quad 10 M_{Sun}, \quad T \approx 10^{7} K$$

Ultra luminous X-ray sources (ULXs):

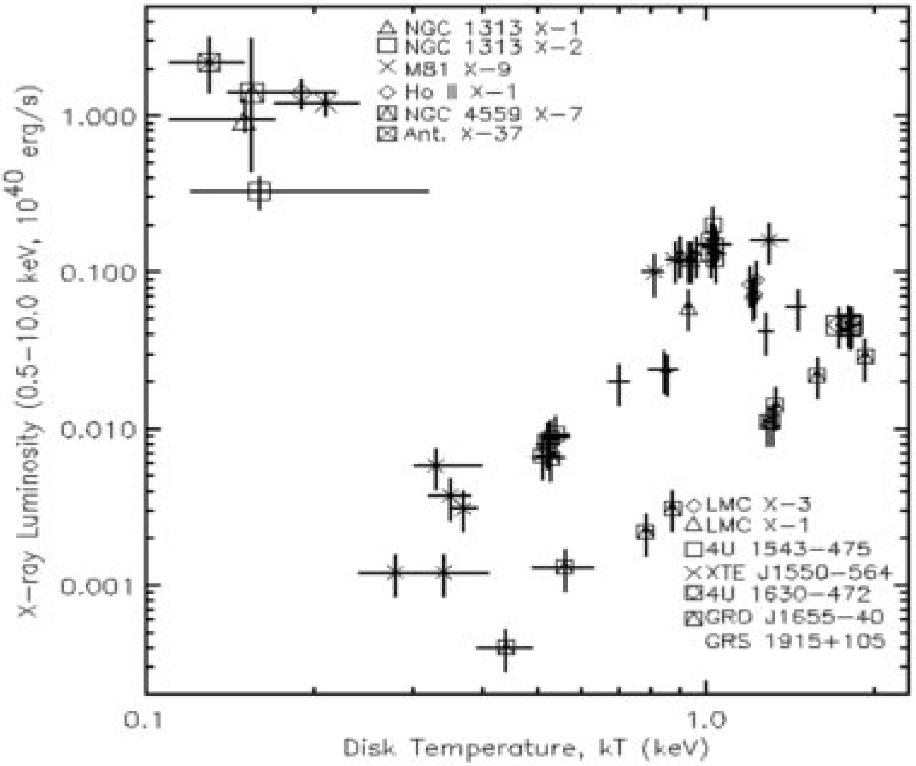

Figure 2. ULXs with cool accretion disks do not lie on the temperature–luminosity trend observed in stellar-mass black holes, and form a rather tight group, suggesting a distinct subclass, which may indeed harbor IMBHs (Miller et al., 2004a).

The disk temperature is lower than in X-ray binaries suggesting lower accretion rate or higher black hole mass.

SMBH – radiatively inefficient flows:

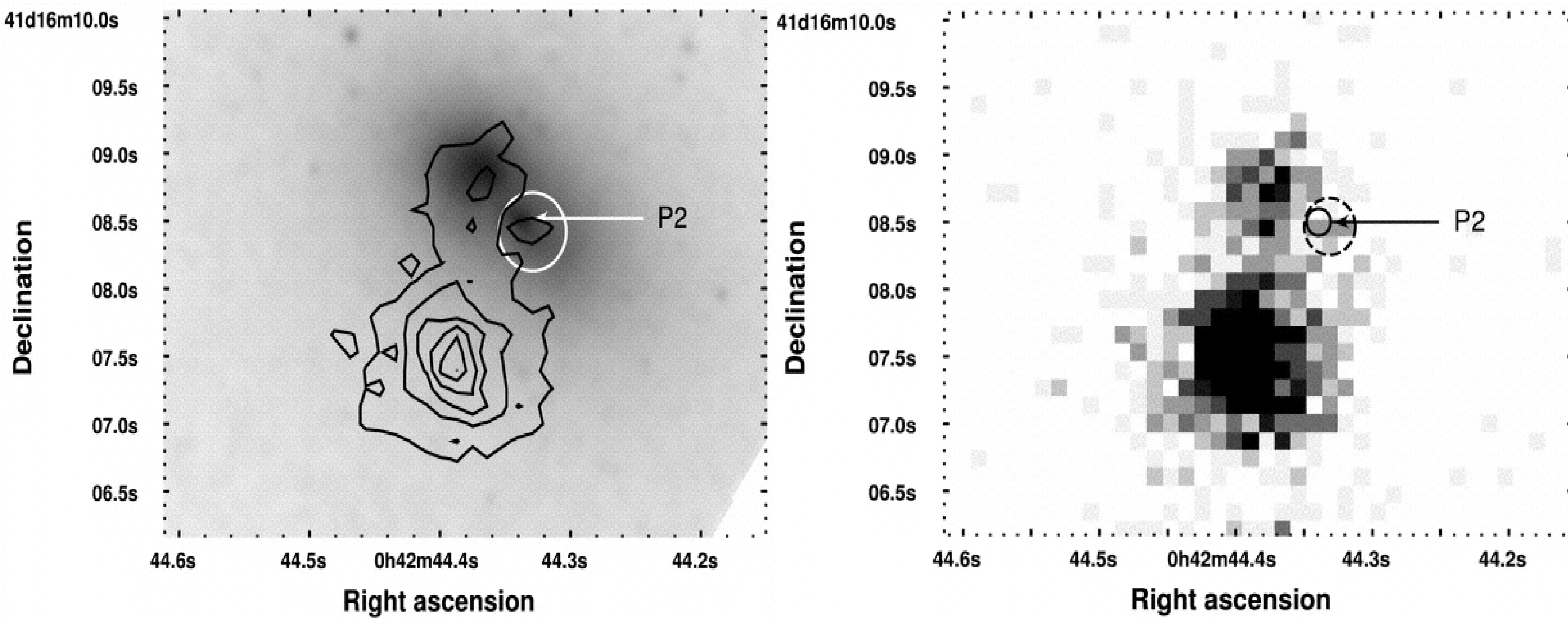

HST (left) and Chandra (right) image of M33 and radio source P2 – possible galactic center. Dashed circle is consistent with the position of the black hole. Only 13 counts were detected within the circle, Garcia+2005.

Hot plasma component:

Fabbiano + 1989, 1992 have systematically analyzed all Einstein galaxy observations. They find normal galaxies of all morphological types as spatially extended sources of X-ray emission with luminosities in the 0.2-3.4 keV in the range:

$$L_X \sim 10^{39} - 10^{42}\, erg/s$$

Spiral galaxies reach only 10^{41} erg/s and are harder then for elliptical.

Hot gaseous component in the ISM – HIM was theoretically predicted as a result of SNRs interaction with ISM.

Hot plasma component:

Magellanic Clouds (MC)
SNRs – squares
XRBs – crossed squares
SSSs – double squares.

Sasaki + 2002

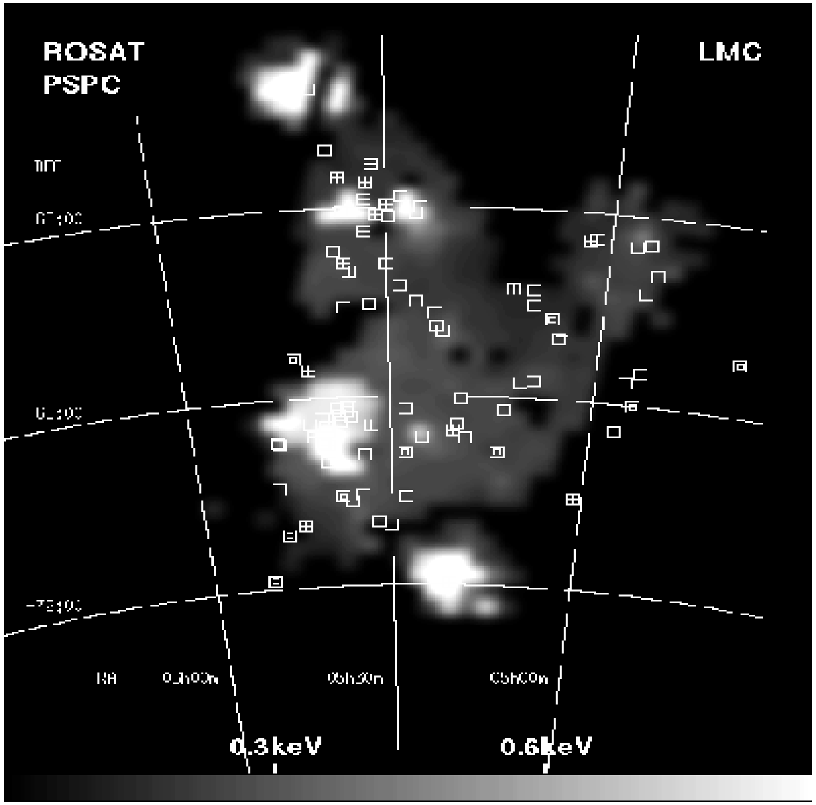

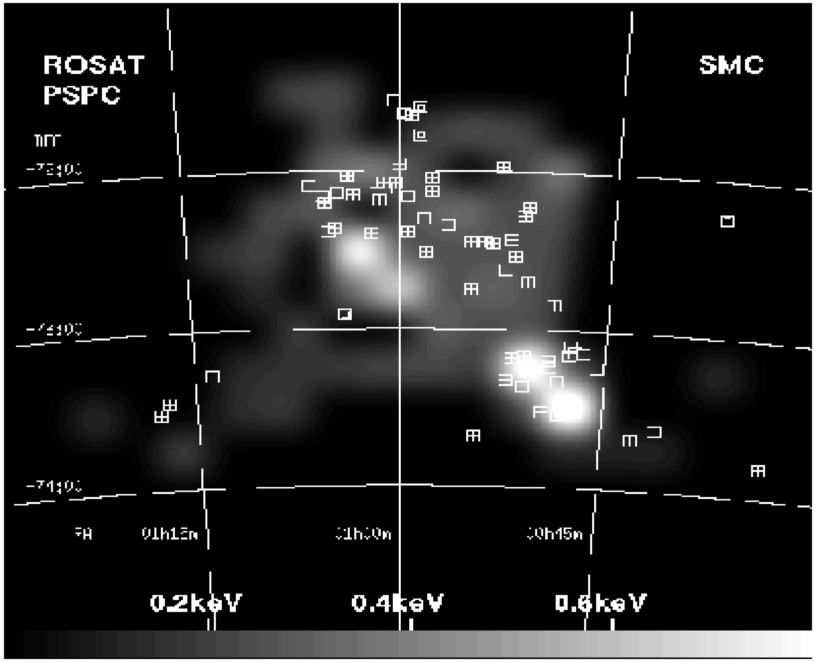

Hot plasma component:

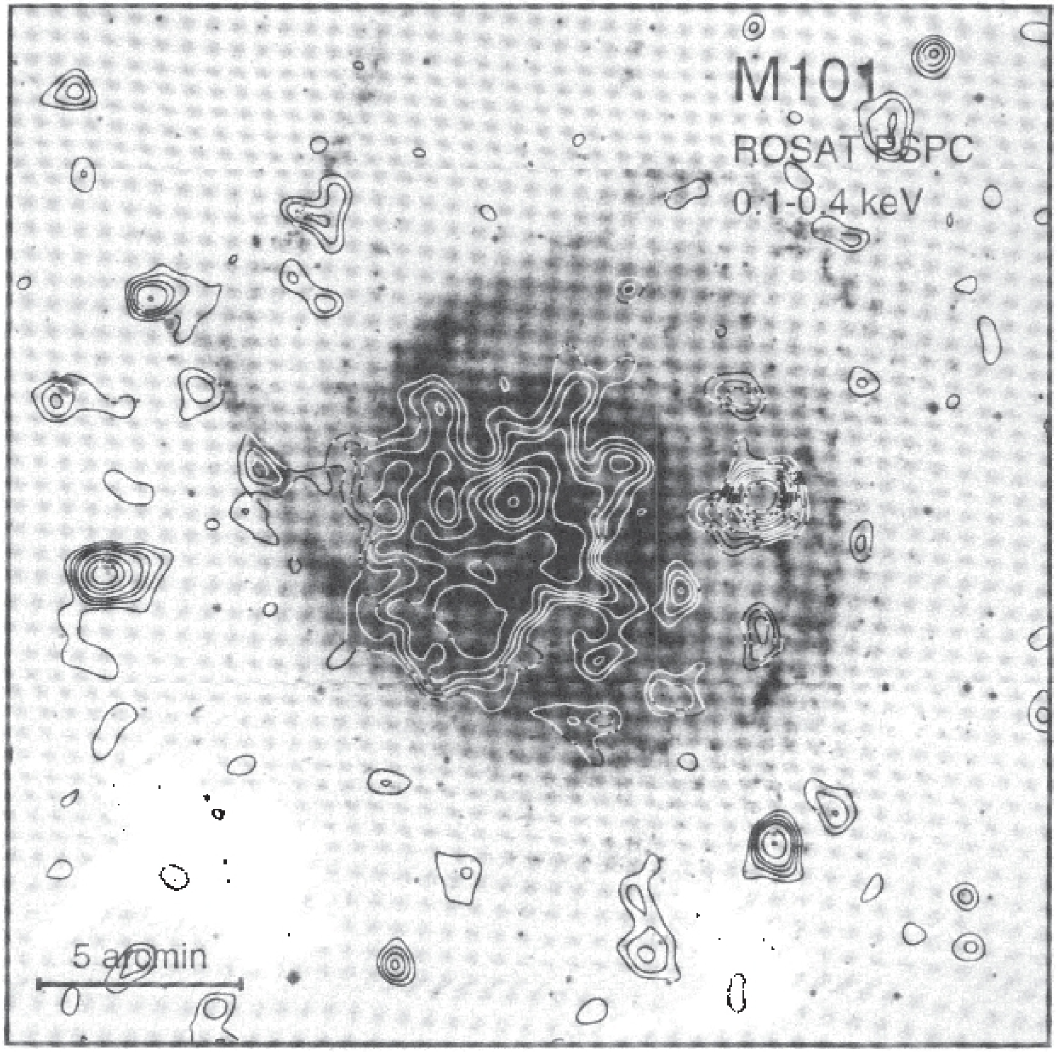

FIG. 2. The $\frac{1}{4}$ keV X-ray contours superposed onto a digitized version of a blue photograph of M101 from the Atlas of Peculiar Galaxies (Arp 1966). X-ray data have been smoothed with a Gaussian function of 42" FWHM. Contours are given for 2, 3, 4, 5, 7, 9, 11, 13, and 17 σ level above background (1 σ corresponds to 220×10^{-6} counts s^{-1} $arcmin^{-2}$).

SNOWDEN & PIETSCH (see 452, 628)

Diffuse X-ray emission from M101.

For the first time ROSAT showed evidence for shadowing of the soft X-ray background at about 0.25 keV by a M101 spiral arm.

Snowden + 1995

Hot plasma component:

XMM-Newton EPIC observations of NGC 253 – starburst galaxy.

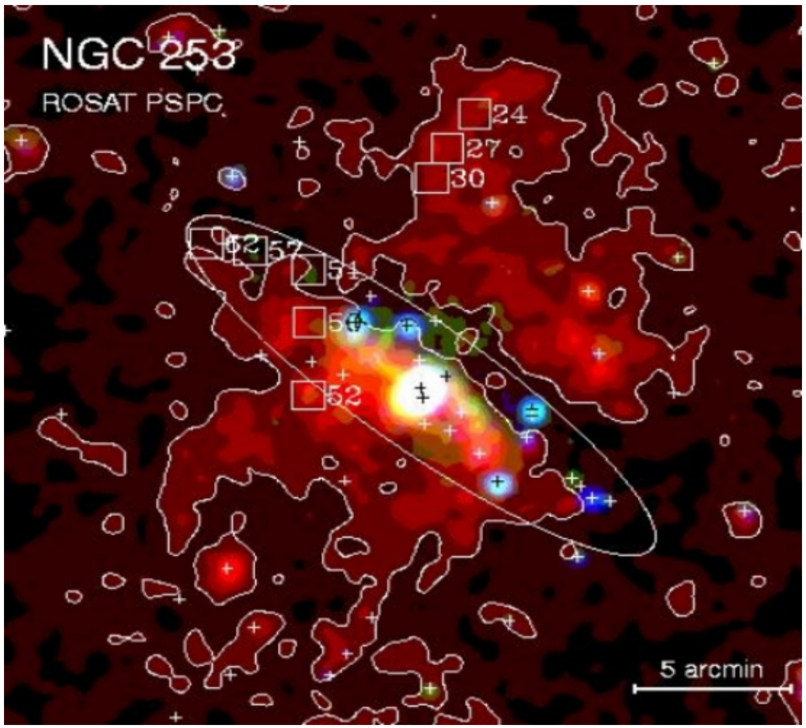

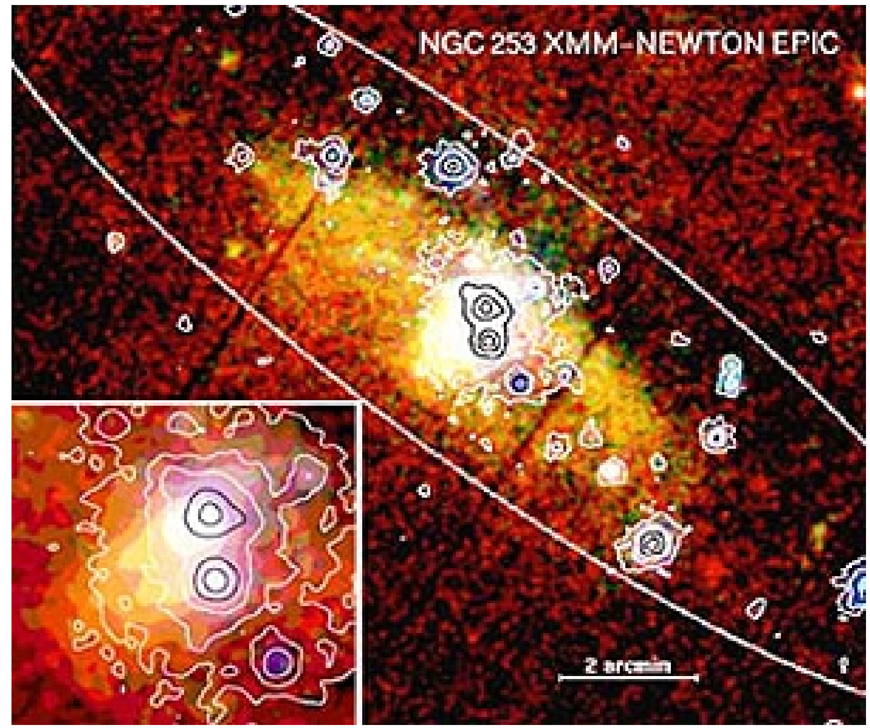

Red – lower energy 0.1-0.5 keV, blue – 1-2 keV. Hard emission 2-10 keV is shown superimposed in the EPIC image as countours. Emission absorbed by ISM, many point-like sources resolved in the disk. The ellipse indicates the optical extent.

Hot plasma component in Centaurus A:

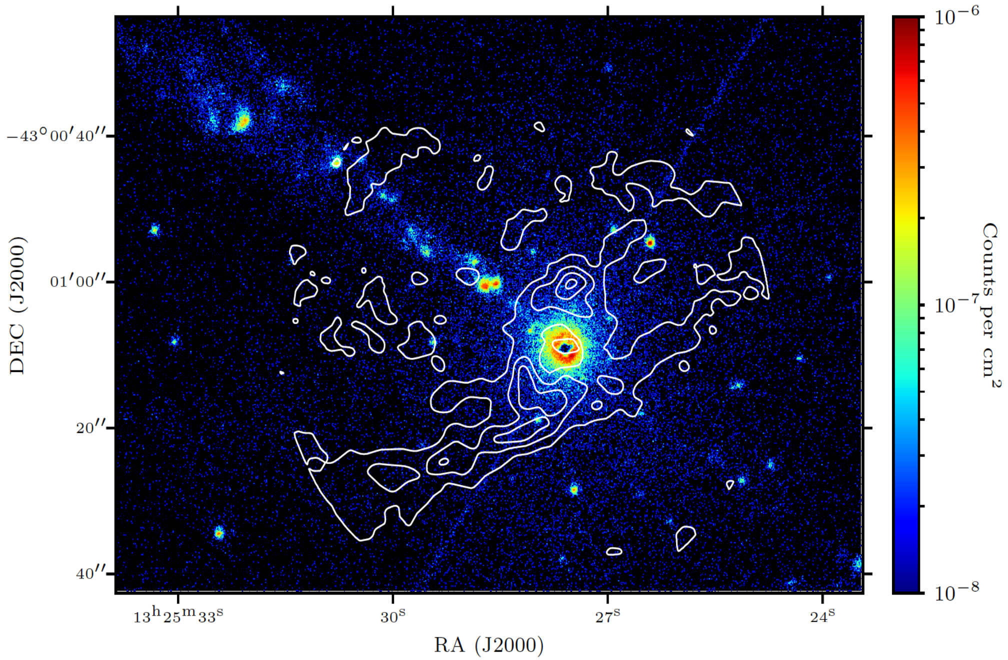

Borkar + 2021

ALMA + Chandra

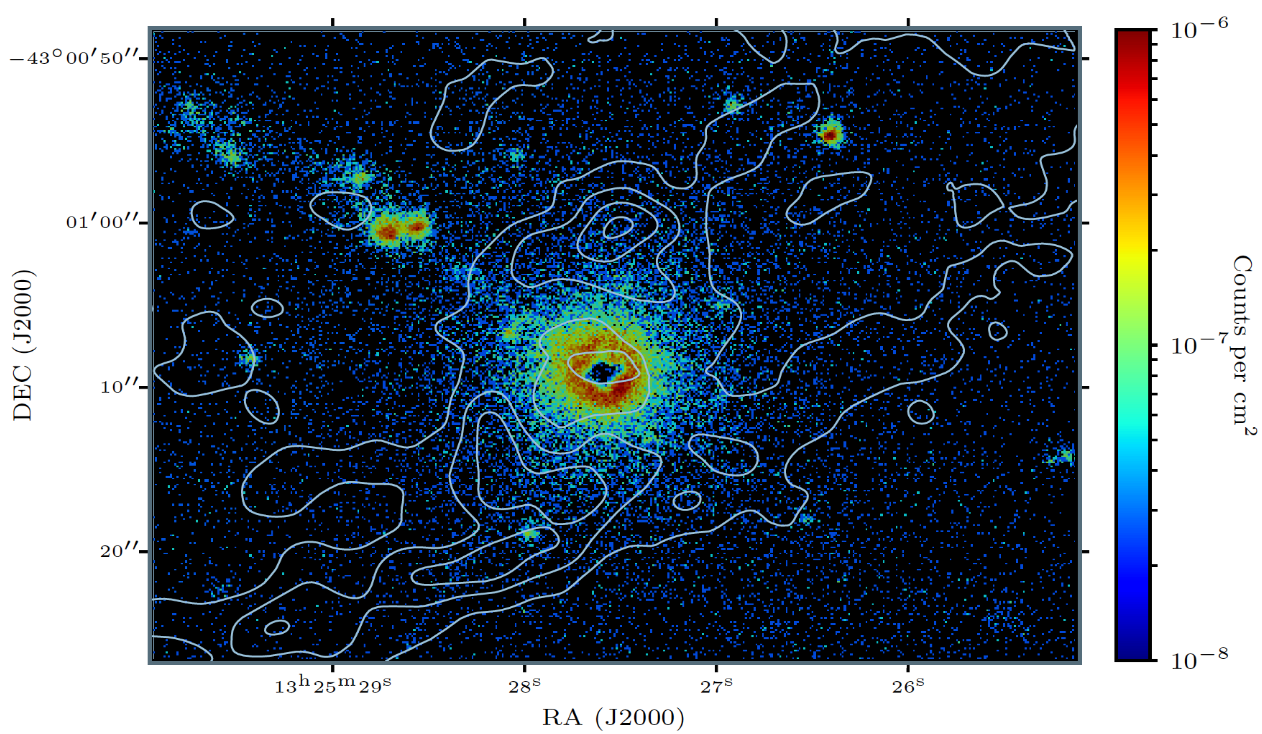

Hot plasma component in Centaurus A:

Borkar + 2021
Simulations of photoionization with CLOUDY code. Gas+Dust

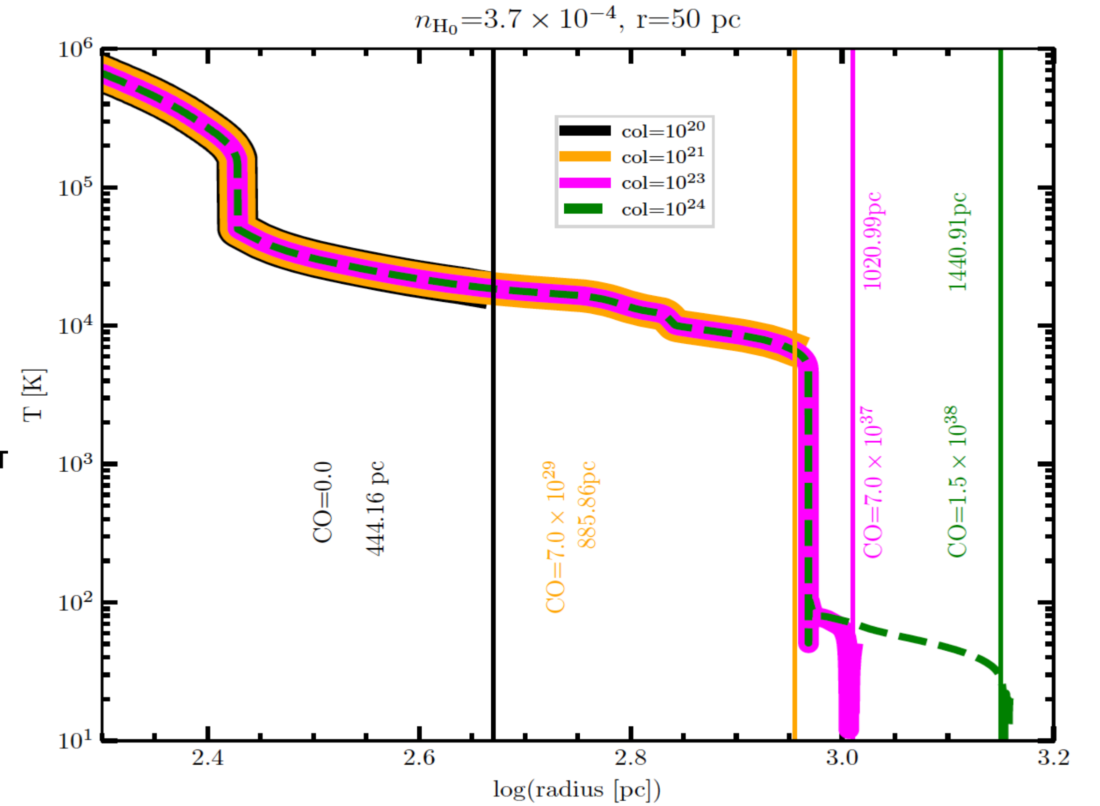

Figure 15. Same as Fig. 14, but for r= 50 pc.

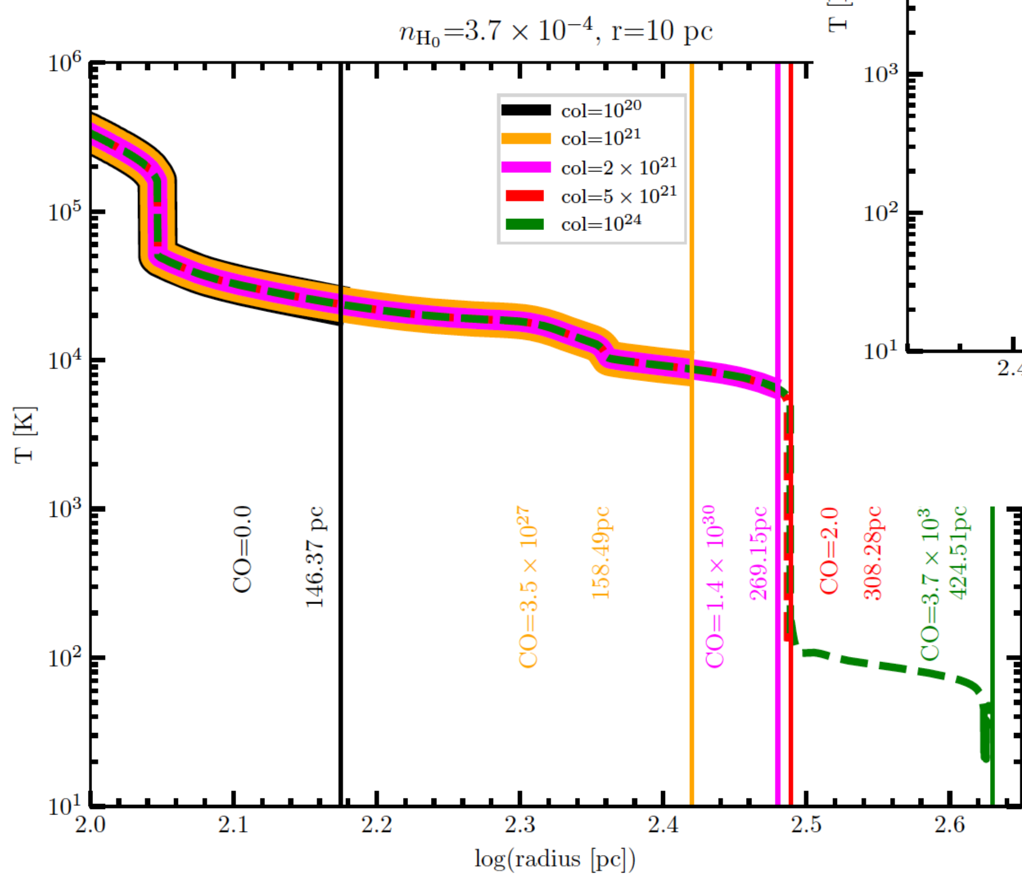

Figure 14. Length scales of CO (1 – 0) emission for various column densities given in the panel box. The model is computed for the gas density: 3.7 × 10^{-4} located at the inner radius 10 pc. For each case the cloud outer radius is marked by a vertical line. The resulting cloud sizes and CO (1 – 0) line luminosities are displayed near each vertical line.

Clusters of galaxies – largest objects in the Universe:

The next to quasars, most luminous X-ray source in the Universe with radiation powers of the order of 10^{43}-10^{46} erg/s.
Hot intraclaster plasma (ICM) with temperatures of few x 10^7 K.
Gives information on the cluster structure since radiation is thermal. X-ray imaging studies of those objects are important.

Coma cluster about: $100\, h_{70}^{-1}\, Mpc$

SDSS

ROSAT 1.42 x 1.42 deg^2

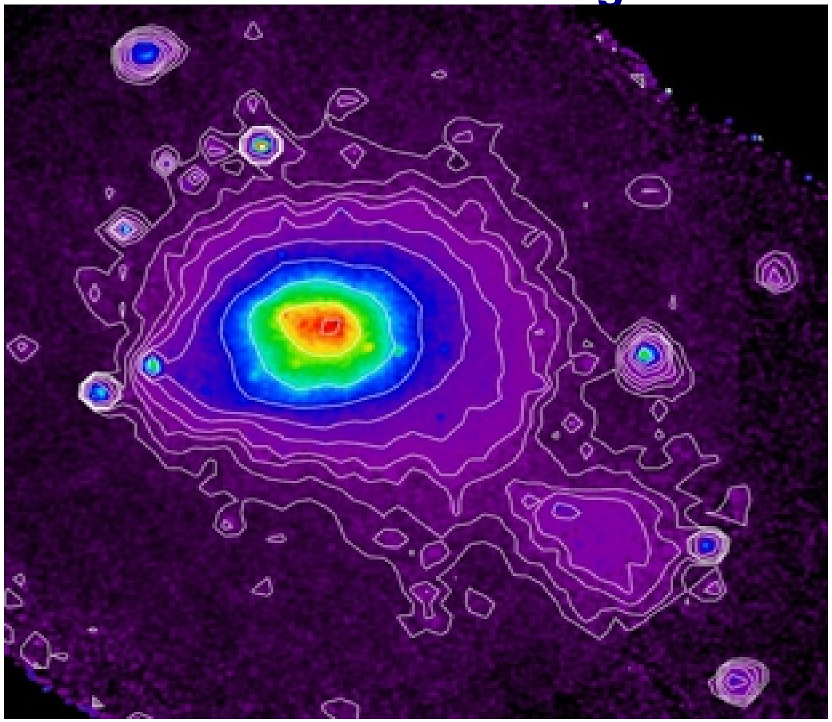

Clusters of galaxies – largest objects in the Universe:

ICM constitutes an atmosphere, which is approximately in hydrostatic equilibrium in the cluster potential:

$$M(r) = -\frac{k_B T(r)}{G \mu m_p} r \left(\frac{d \log(\rho)}{d \log(r)} + \frac{d \log(T_X)}{d \log(r)} \right)$$

where, mp is a proton mass, μ is the mean molecular particle weight (~ 0.6 for fully ionized ICM plasma). From observations we get T_X (r) and ρ(r) profiles.

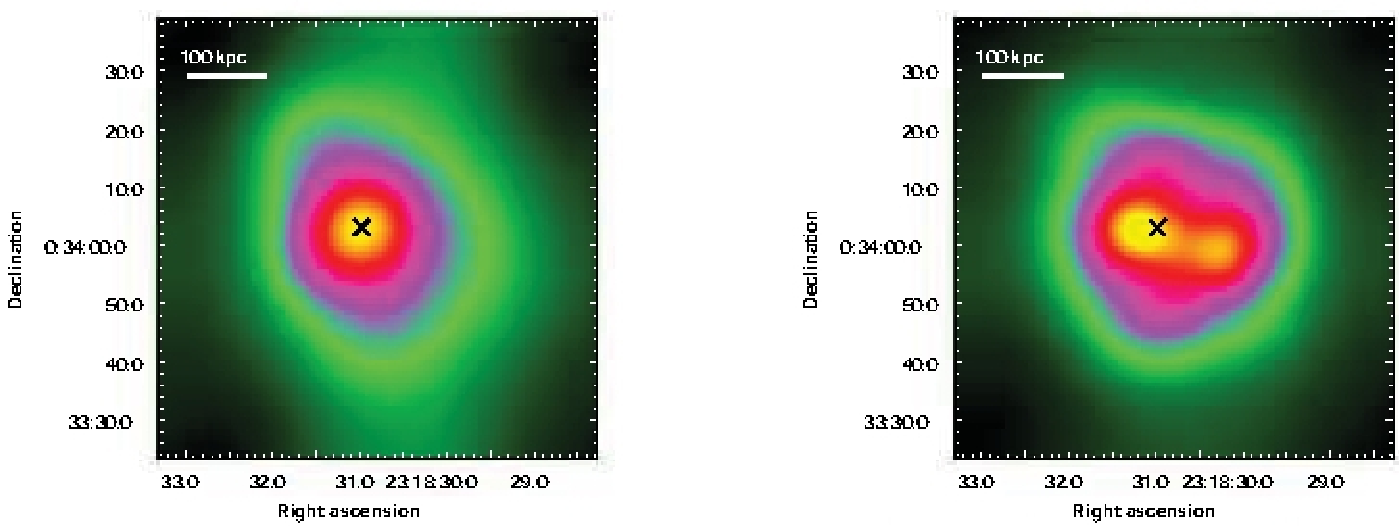

FIG. 1.— left: hard band (2.0-6.0 keV) adaptively smoothed image, and right: soft band (0.5-2.0 keV) adaptively smoothed image of RCS 2318+0034. The cross marks the location of the peak surface brightness of the main cluster in the hard band image.

RCX2318+0034
Chandra
Laurence+ 2012

2.0-6.0 keV – left

0.5-2.0 keV – right.

Clusters of galaxies – largest objects in the Universe:

ICM constitutes an atmosphere, which is approximately in hydrostatic equilibrium in the cluster potential:

$$M(r) = -\frac{k_B T(r)}{G \mu m_p} r \left(\frac{d \log(\rho)}{d \log(r)} + \frac{d \log(T_X)}{d \log(r)} \right)$$

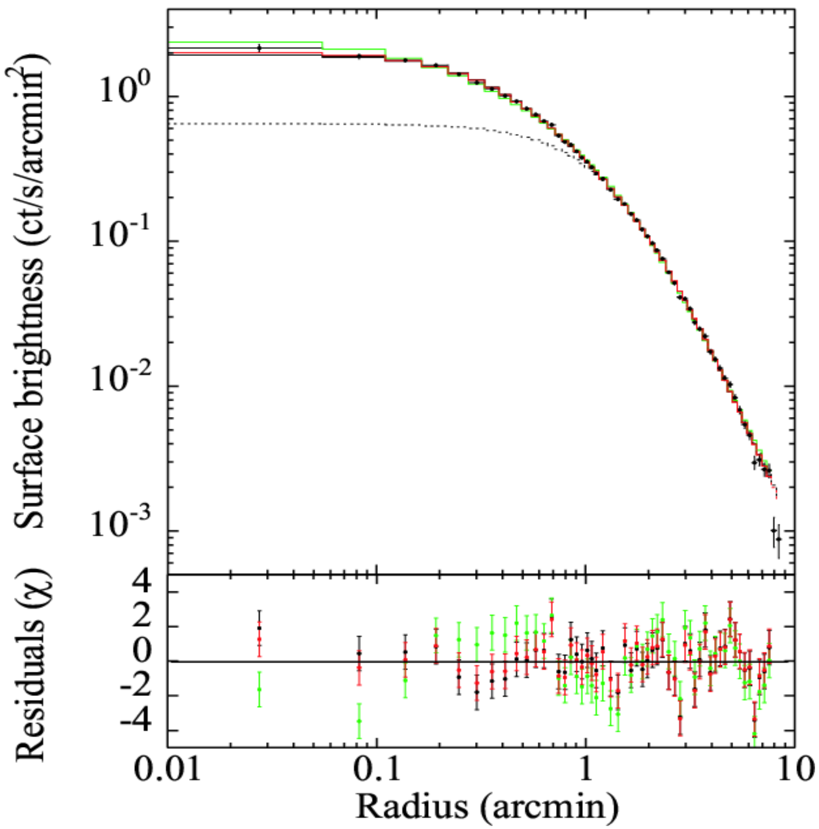

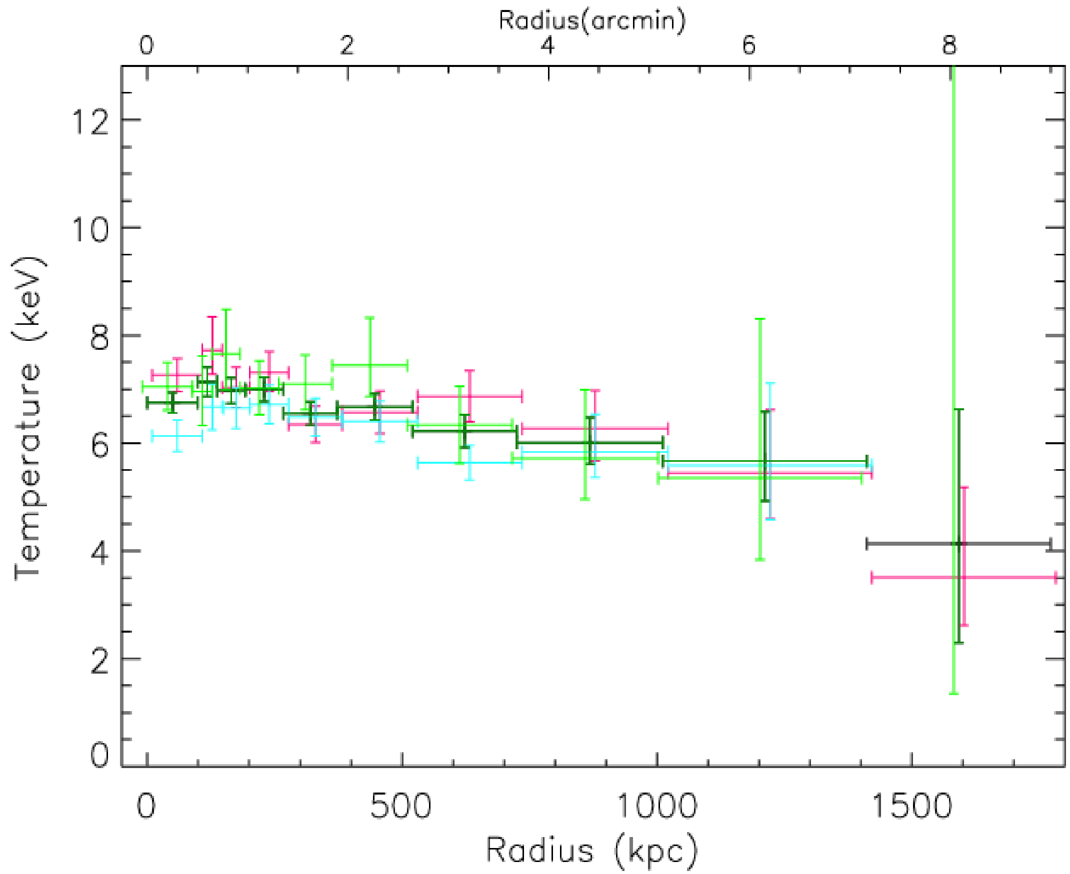

Abel 1413

Clusters of galaxies – largest objects in the Universe:

ICM constitutes an atmosphere, which is approximately in hydrostatic equilibrium in the cluster potential:

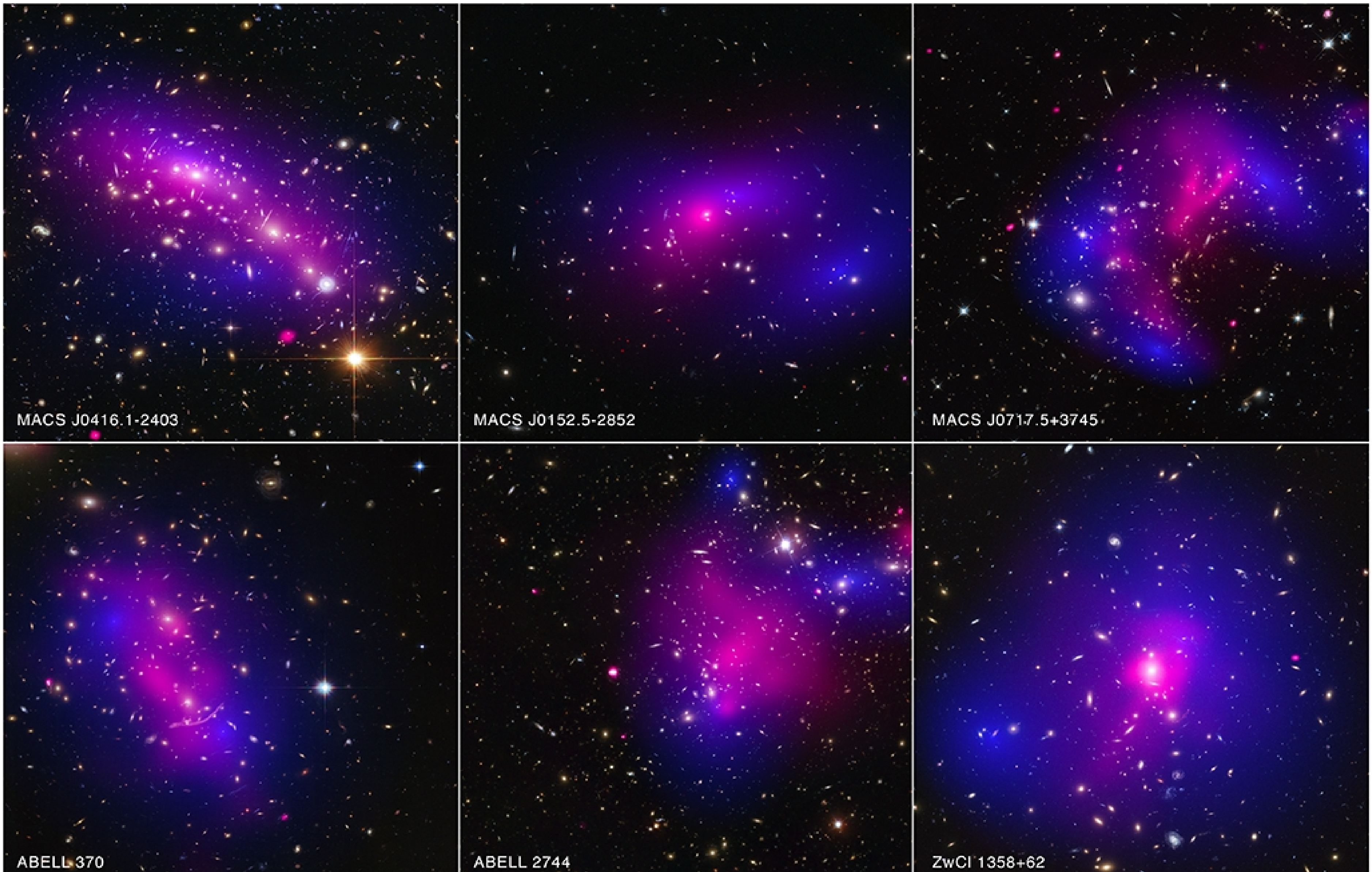

Clusters of galaxies – largest objects in the Universe:

ICM constitutes an atmosphere, which is approximately in hydrostatic equilibrium in the cluster potential:

Density profiles from N-body simulations Navarro + 1997, or Morre + 1999.

Commonly used density profile:

$$\rho_{\rm gas}(r) = \rho_{\rm gas}(0)\left[1 + \left(\frac{r}{r_c}\right)^2\right]^{-\frac{3}{2}\beta},$$

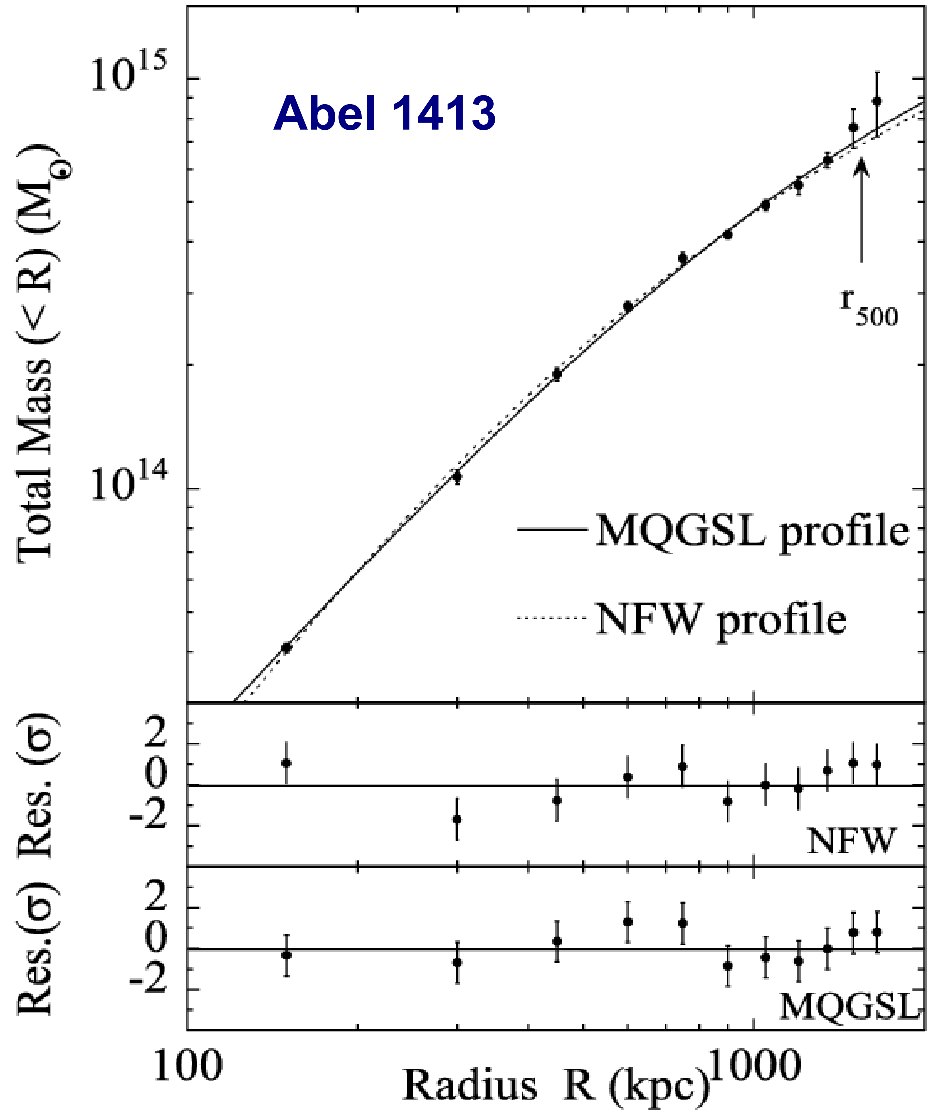

Clusters of galaxies – largest objects in the Universe:

The X-ray emitting ICM is the largest visible matter component, 5-6 times larger than optical part.
Gas mass fraction about 12% of total mass of the cluster:

$$\frac{M_{gas}}{M_{tot}} = 0.207 \pm 0.037 h_{50}^{-3/2} = \frac{\Omega_b}{\Omega_m} = \frac{0.08 \pm 0.008 h_{50}^{-2}}{\Omega_m}.$$

RCX2318+0034
Chandra
Laurence+ 2012

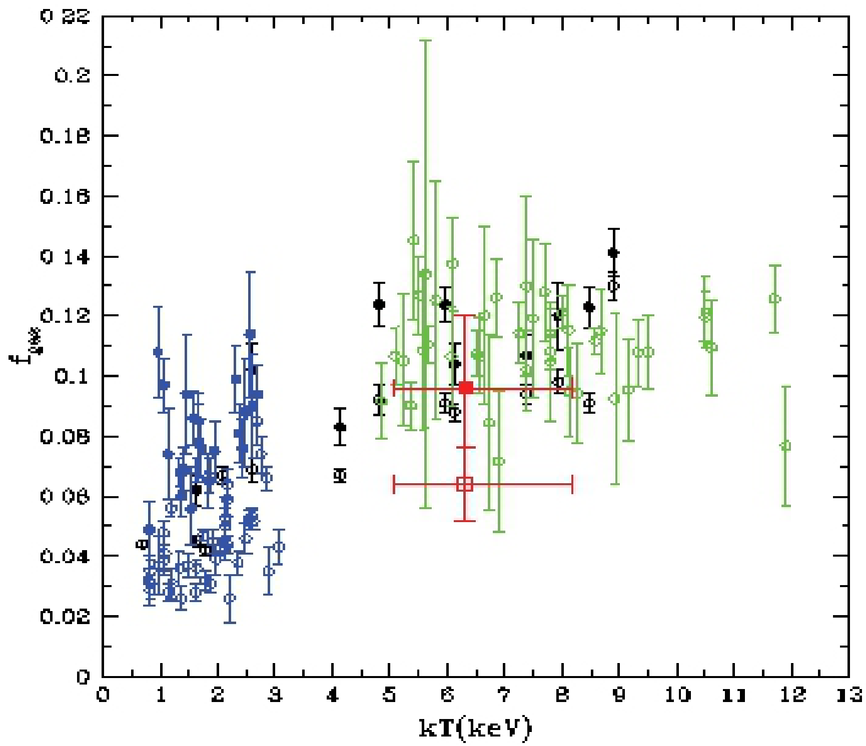

FIG. 6.— Gas mass fractions from Sun et al. (2009) (blue), Vikhlinin et al. (2006) (black), Allen et al. (2008) (green) and RCS 2318+0034 (red). Open symbols give f_{gas} within r_{2500} and solid symbols give f_{gas} within r_{500}.

Clusters of galaxies – largest objects in the Universe:

RCX2318+0034 **Chandra** **Laurence+ 2012**

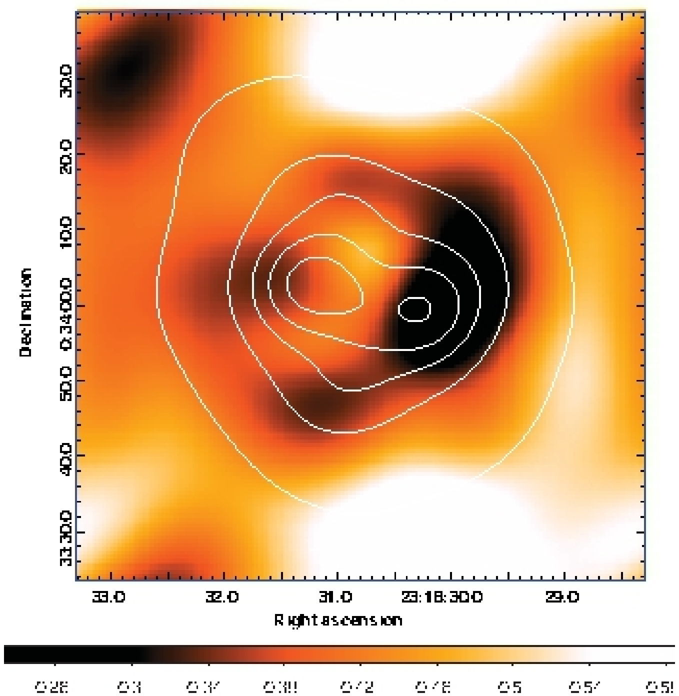

FIG. 2.— Hardness ratio image along with surface brightness contours derived from the soft band image shown in Fig. 1.

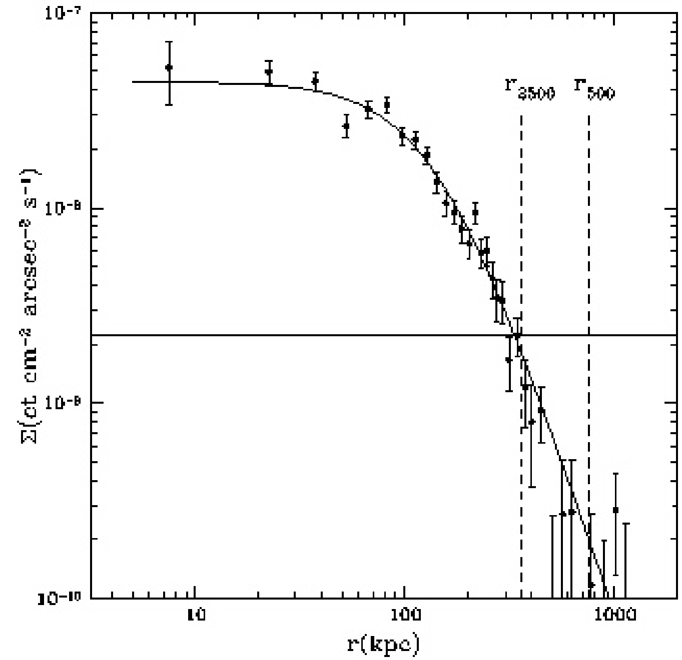

FIG. 3.— Background-subtracted and exposure-corrected 0.3-6.0 keV surface brightness profile of RCS 2318+0034 excluding the emission from a 120° pie slice toward the west along with our standard β model (solid line). Also shown are the ACIS-I background (horizontal solid line) and r_{2500} and r_{500} (vertical dashed lines).

Hardness ratio F(0.5-2)/F(2-6)

r(500) – radius within which the average density of the cluster is 500 times the critical density of the Universe at the redshift of the cluster.

Clusters of galaxies – largest objects in the Universe:

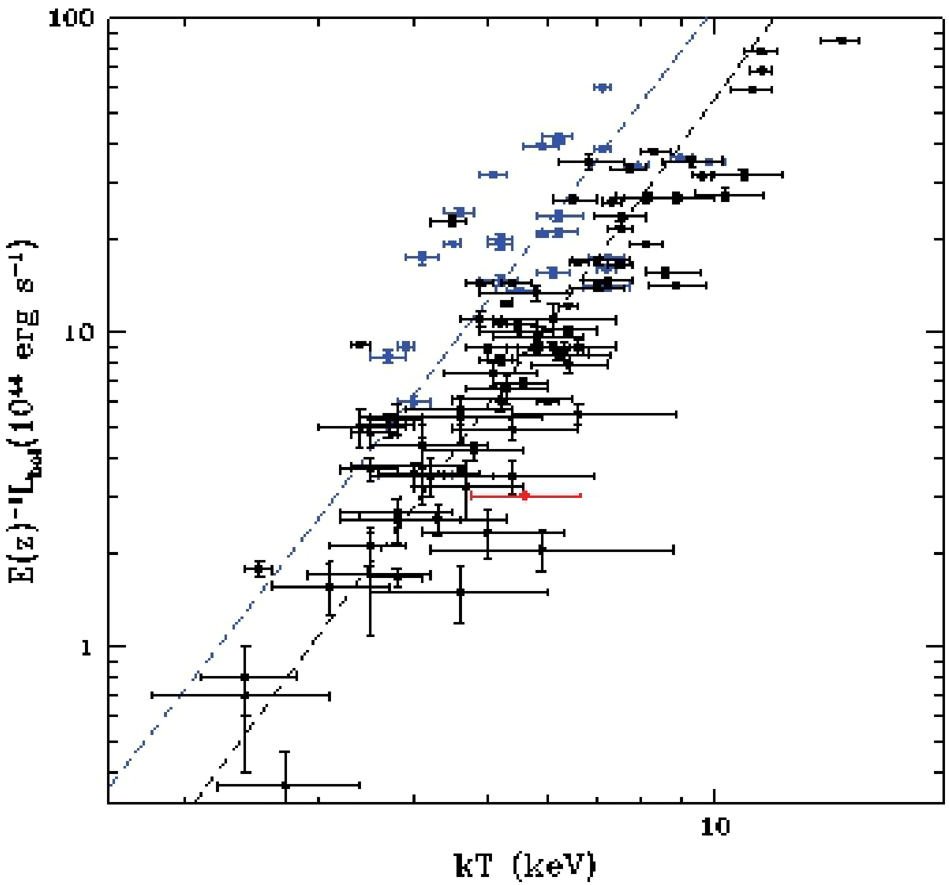

FIG. 8.— Bolometric X-ray luminosity vs. cluster temperature relation for the total emission within r_{500}. The RCS 2318+0034 data point is shown in red. All other data points are from Maughan et al. (2011). Relaxed clusters are shown in blue and unrelaxed clusters are shown in black. Also shown are the best fit relations for relaxed clusters (dashed blue line) and unrelaxed clusters (dashed black line) derived in Maughan et al.

The bolometric luminosity within r(500).

Laurence+ 2012

Cooling and heating of the ICM

Cooling time of the gas falls below the Hubble time.
M87 in Virgo cluster observed by XMM-Newton Bohringer + 2001

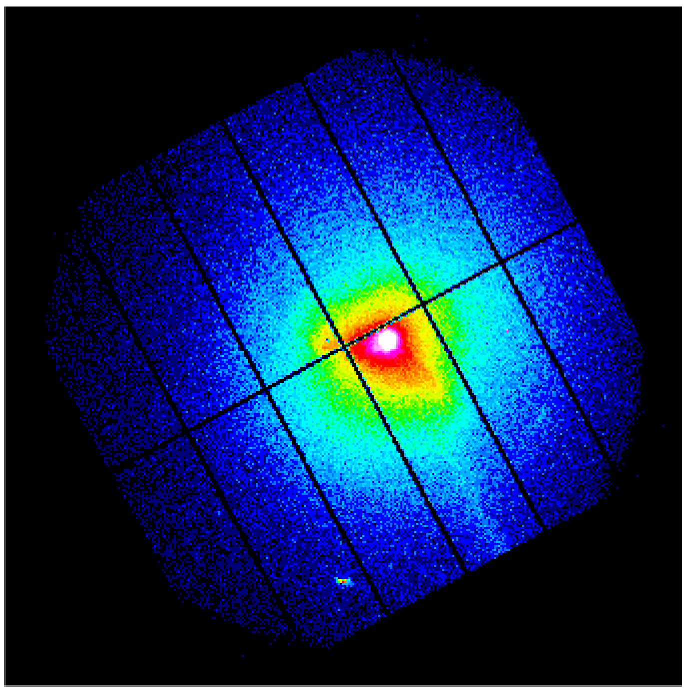

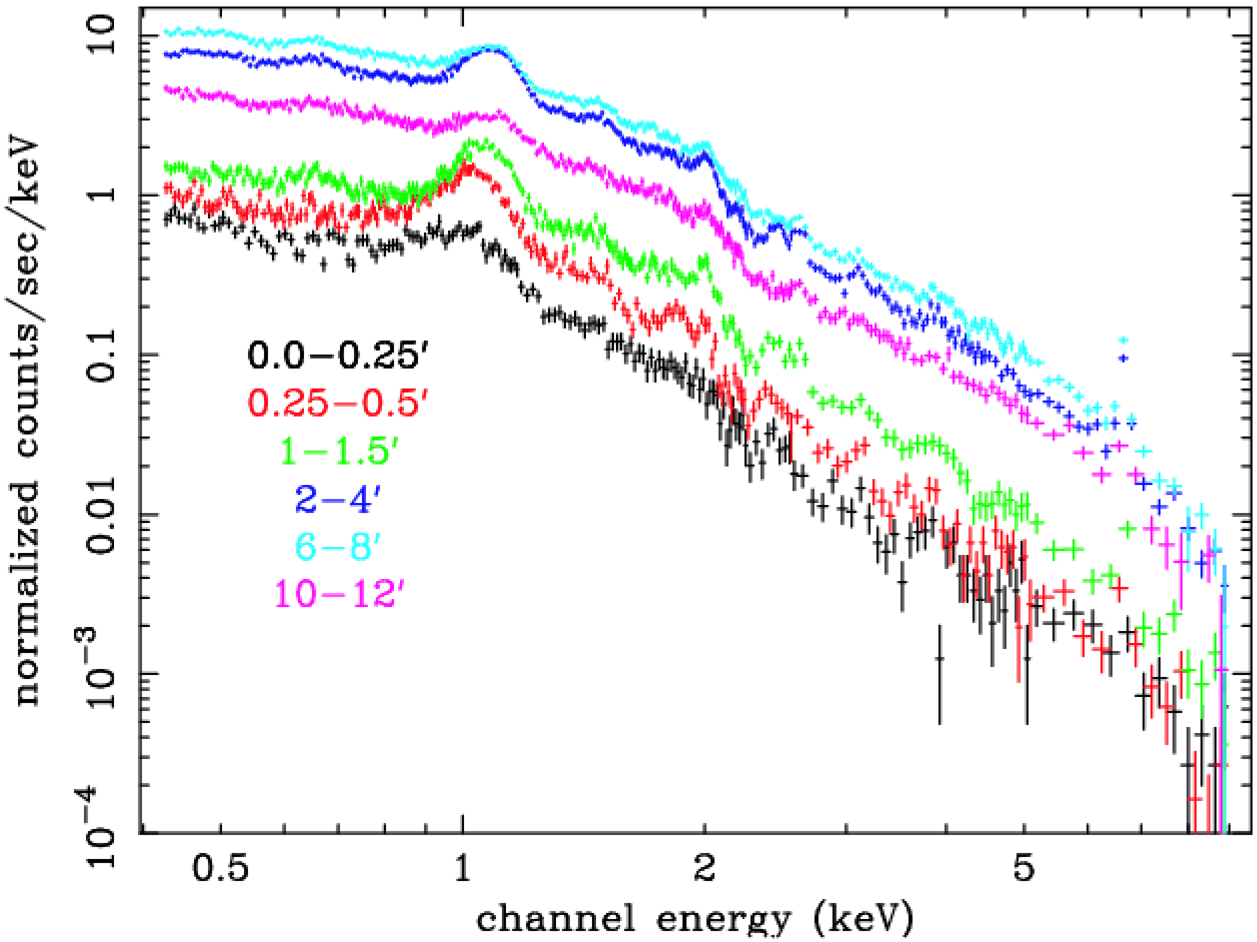

Spectra taken from concentric rings around the nucleus.

Cooling and heating of the ICM

Multi – temperature cooling flow was proposed by Fabian + 1984

Bohringer + 2001

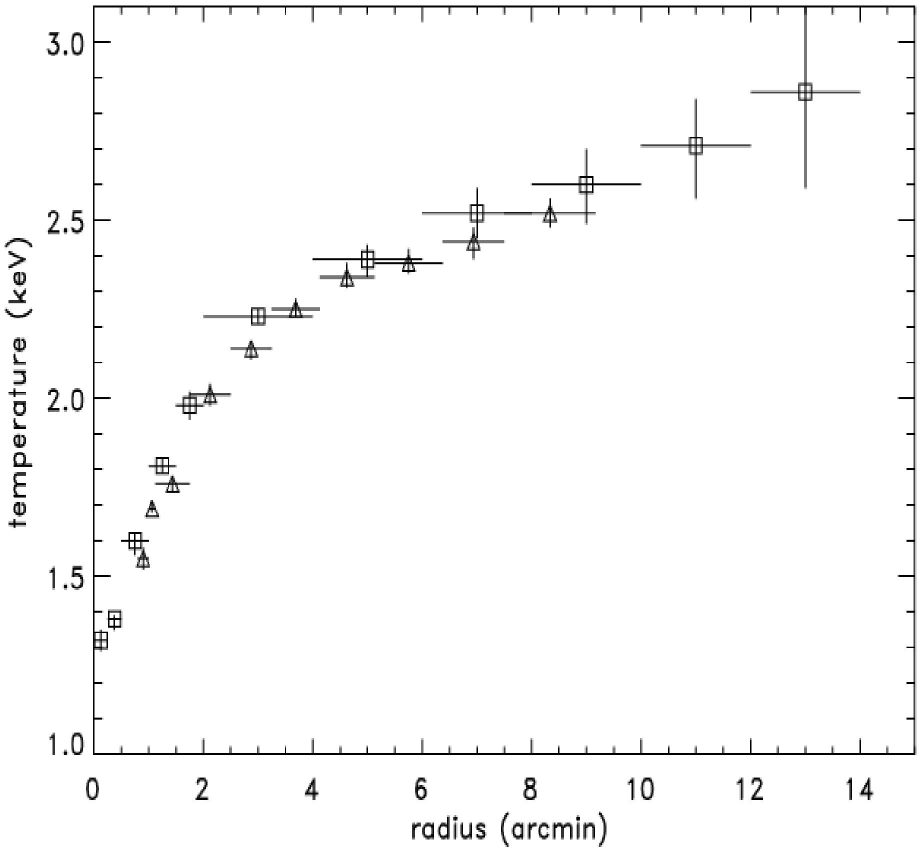

XMM-Newton temperature map

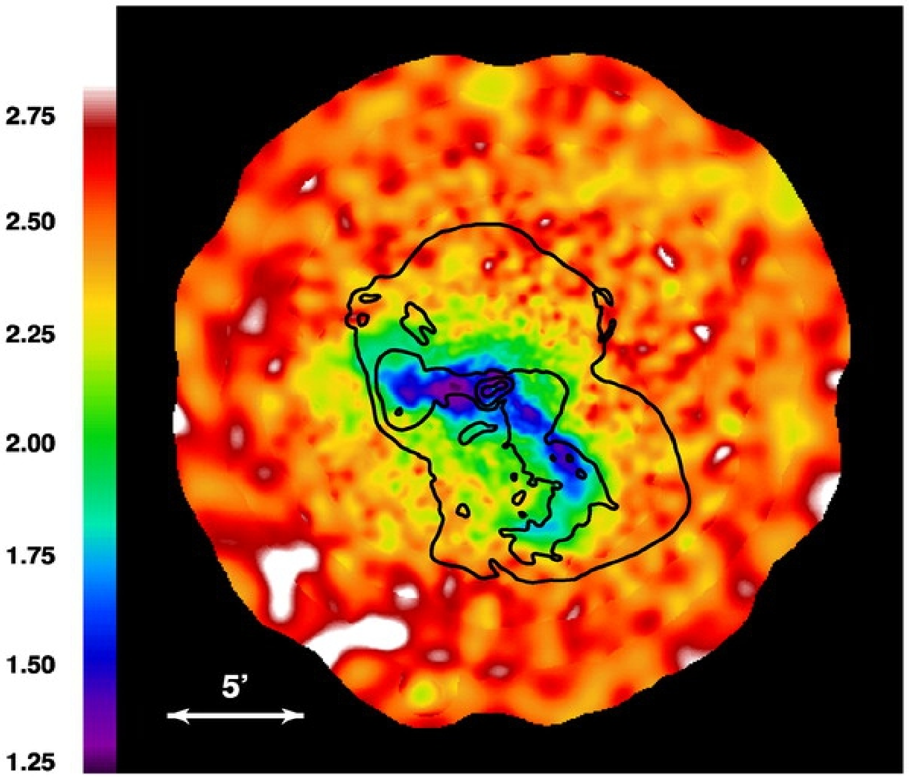

But no lines from low ionization spacies were detected.

Heavy elements enrichment of the cluster ICM:

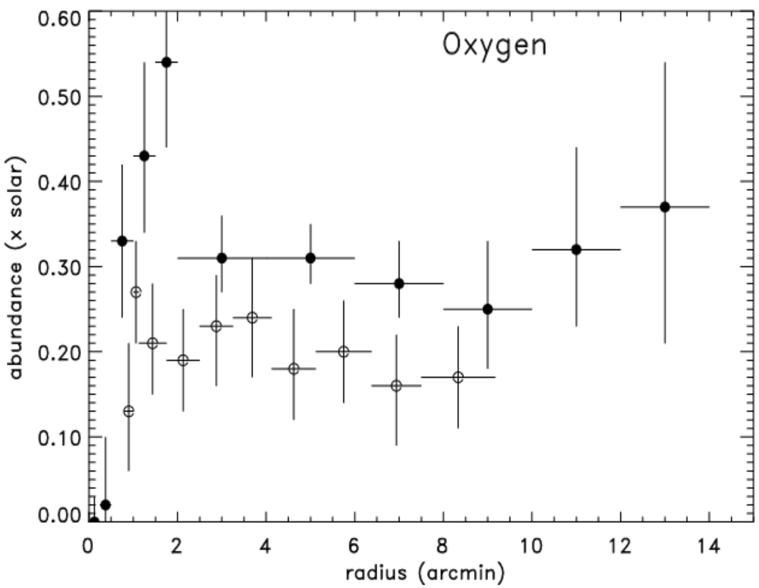

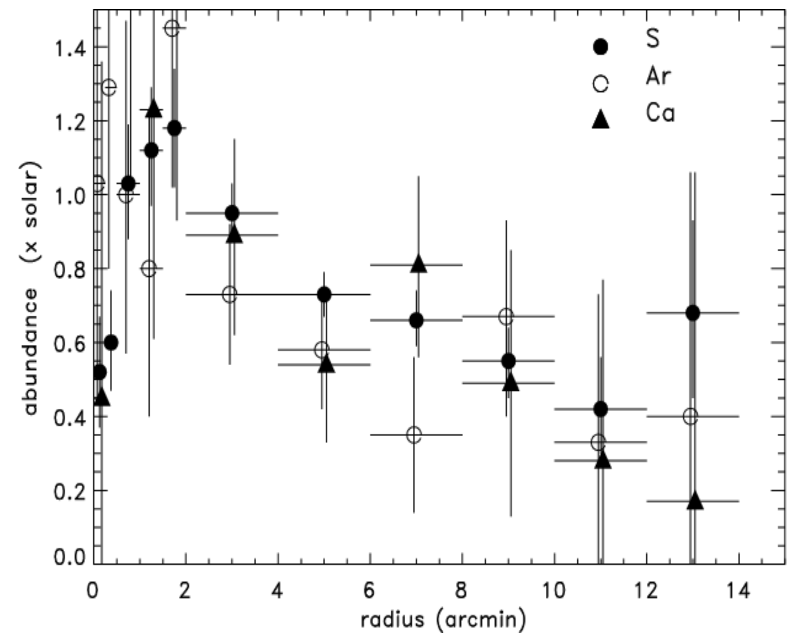

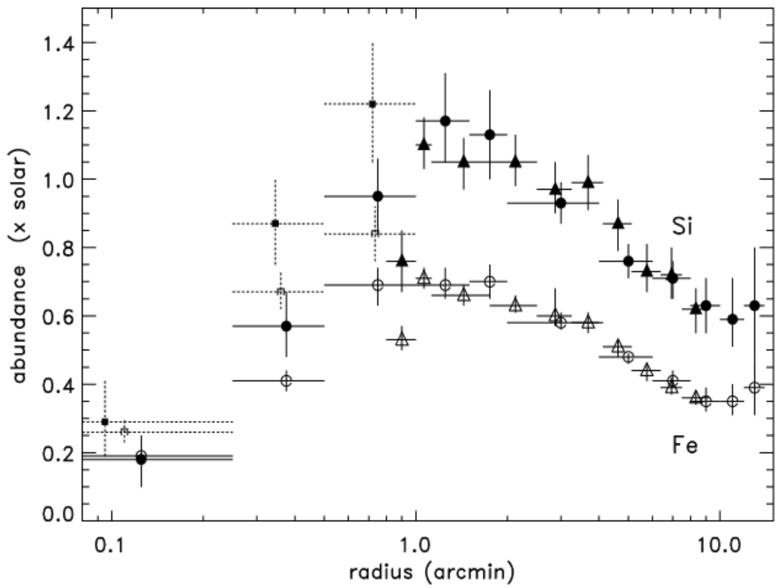

Consistent with SN II activity in the early history of cluster formation.

M87 Bohringer + 2001

Heavy elements enrichment of the cluster ICM:

HITOMI mission operated only one month, Nature 2016

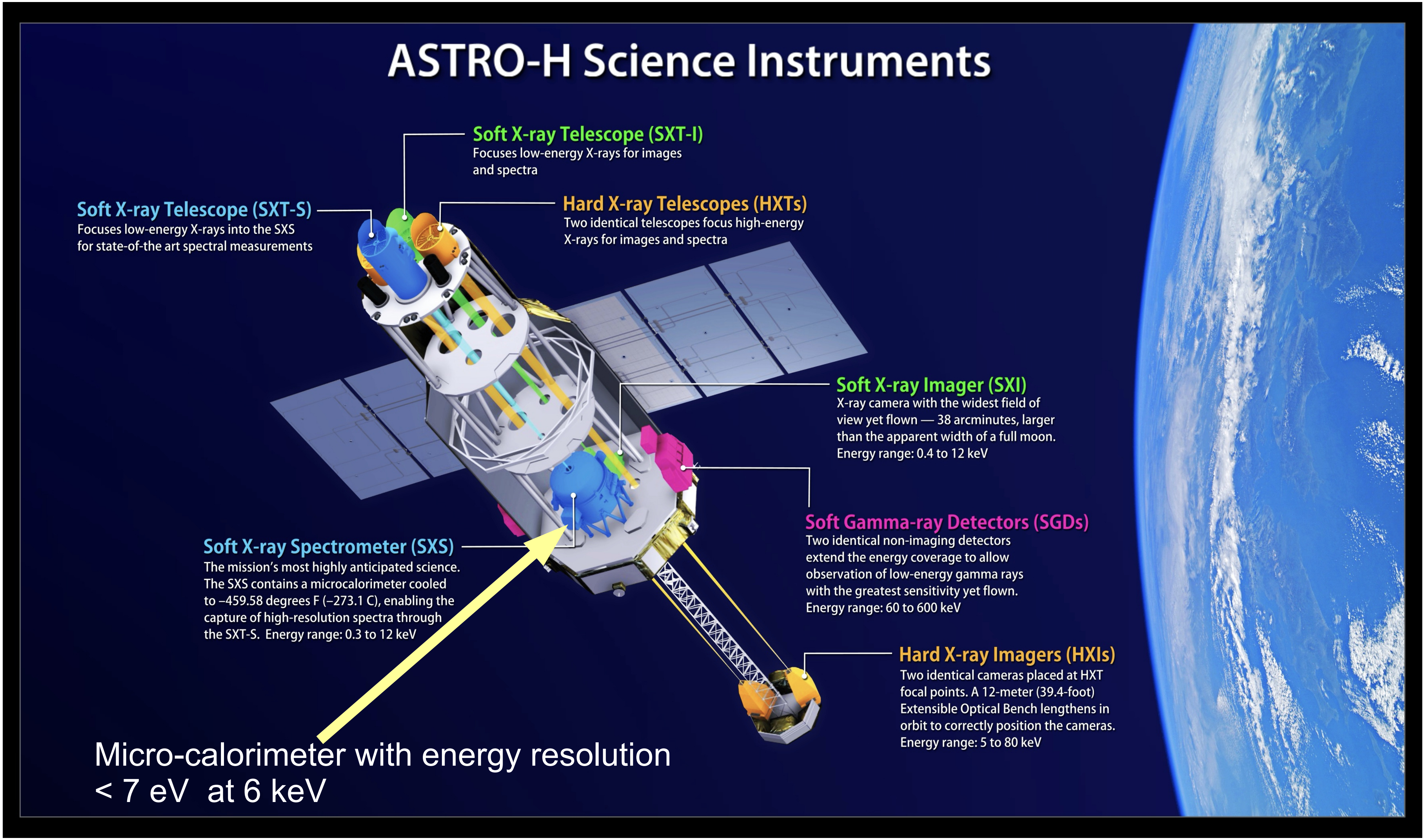

Heavy elements enrichment of the cluster ICM:

HITOMI mission operated only one month, Nature 2016

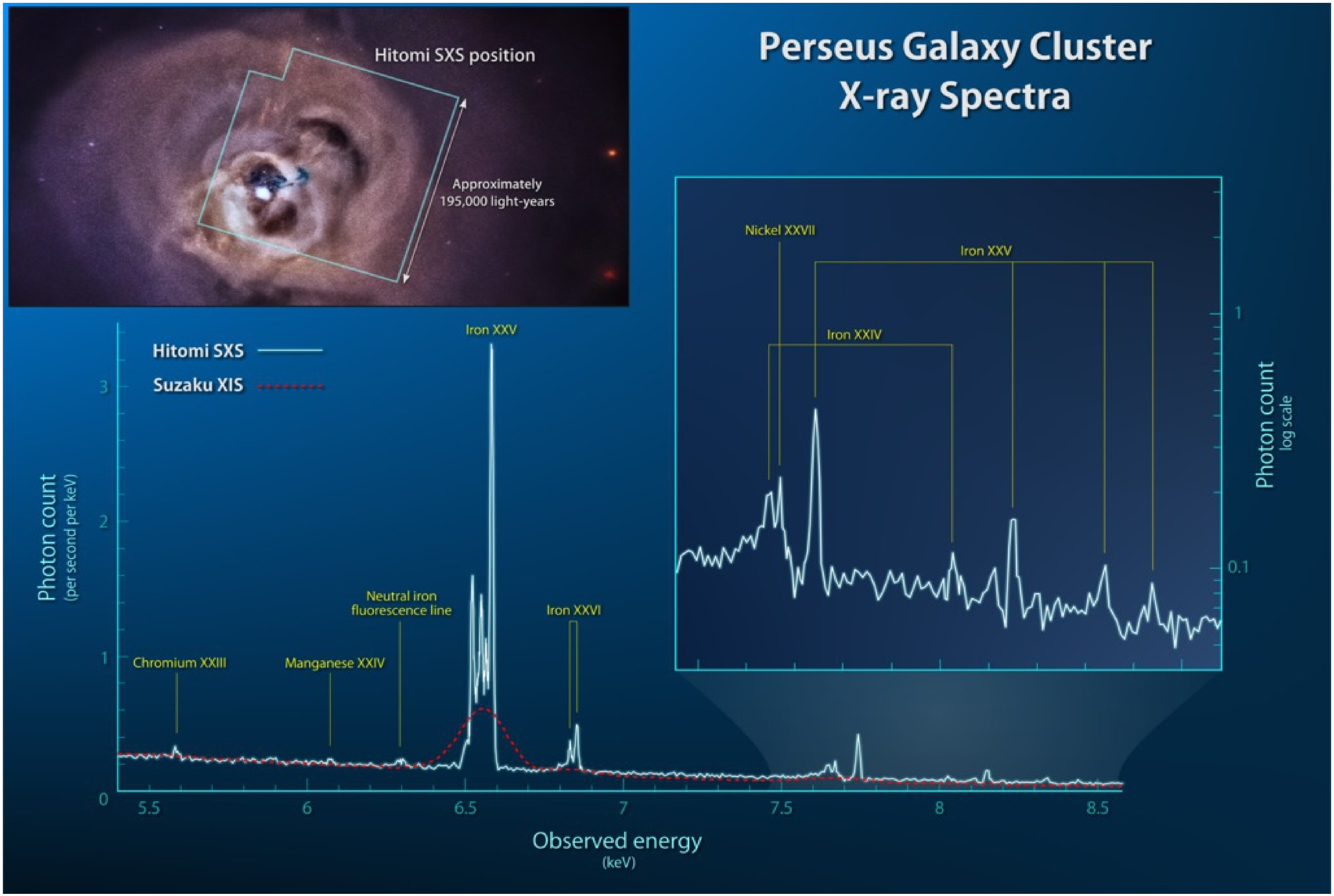

Heavy elements enrichment of the cluster ICM:

HITOMI mission operated only one month, Nature 2016

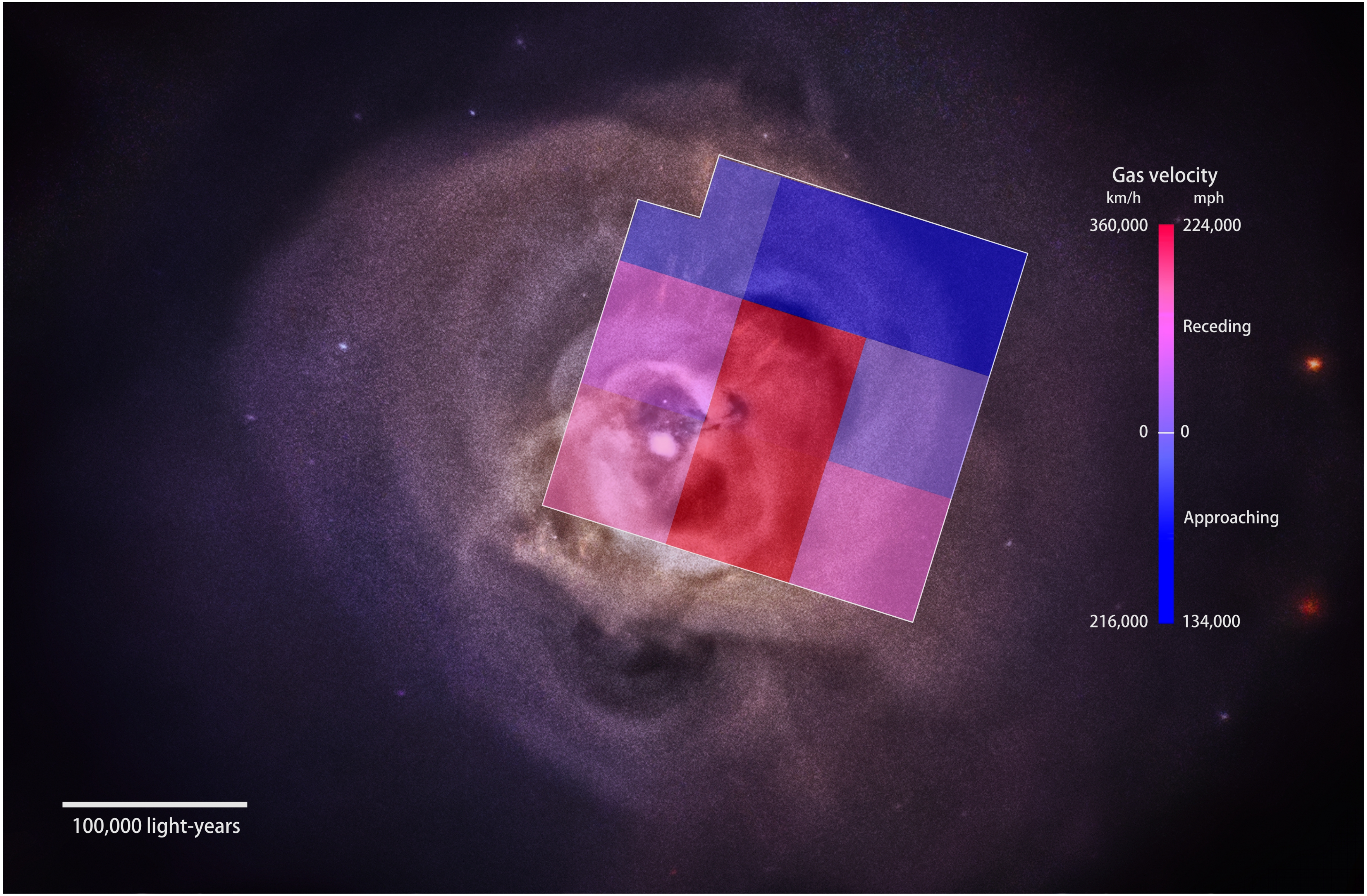

Cooling and heating of the ICM - Galaxy Feedback

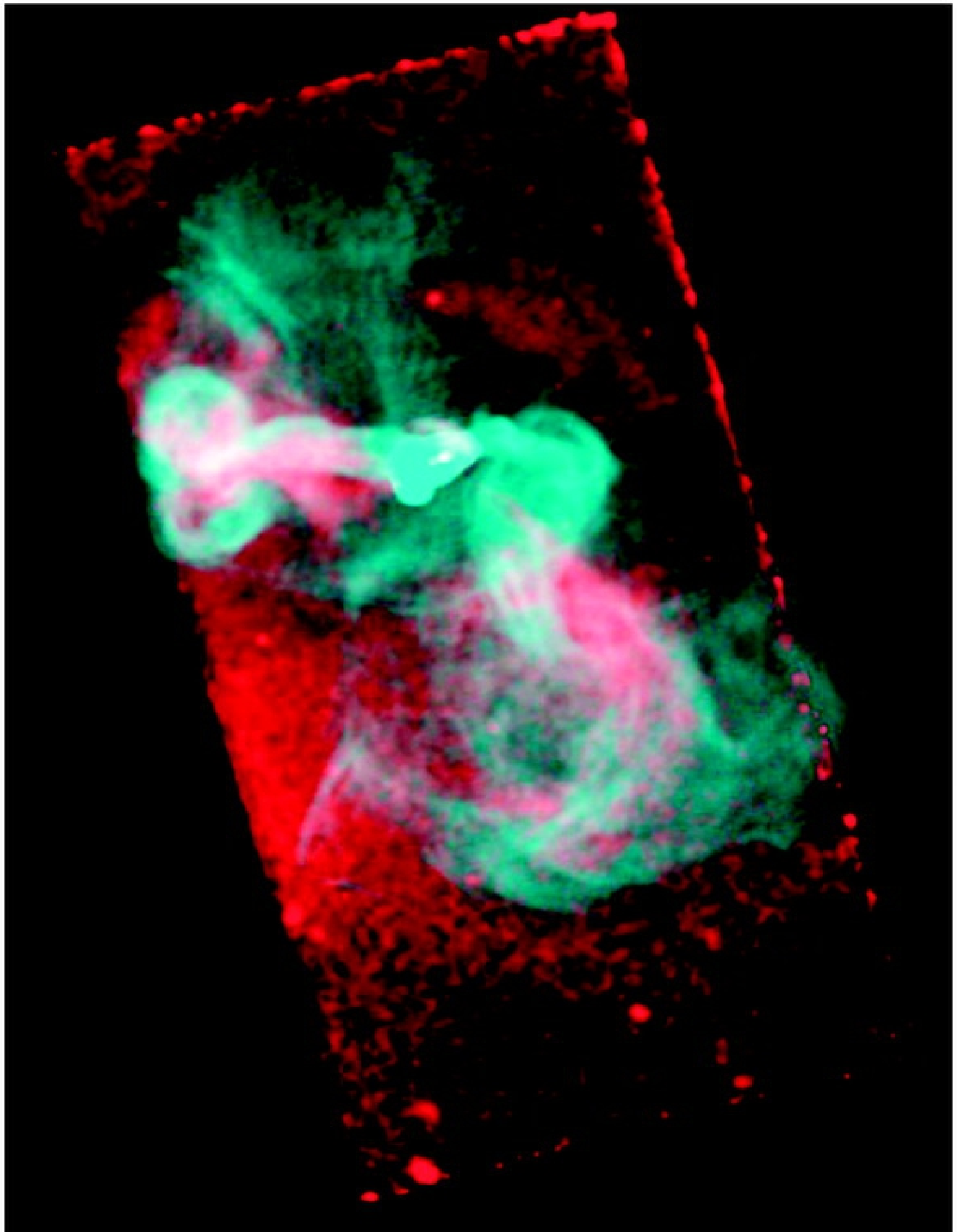

Composite image of the M87 halo region with X-ray emission in red and radio emission in blue color.

Impact of Active Galactic Nucleus outburst in its gaseous atmosphere.

Warm Hot Intergalactic Medium - Galaxy Feedback

Current cosmological model:
The density of matter and energy in the Universe from PLANCK

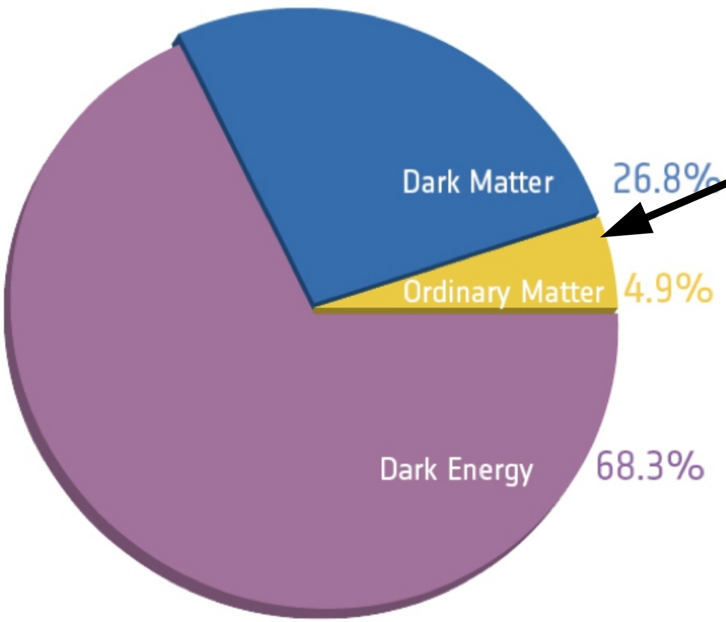

Baryonic matter which we can observe

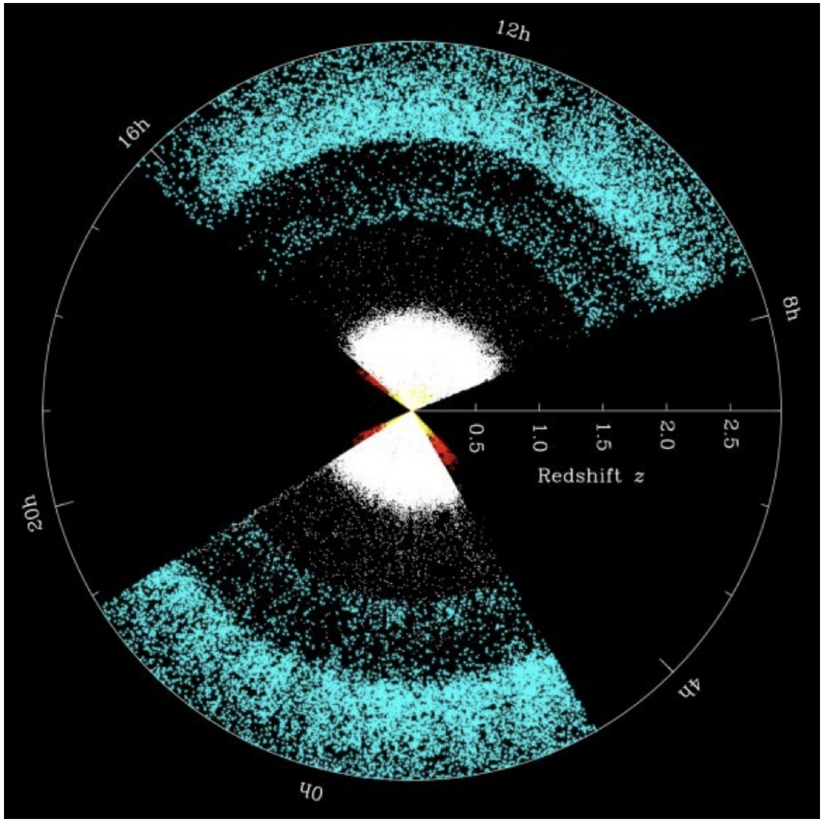

Observed Baryonic matter – 4.9 % in the Universe:

Budget from Shull et al (2012)

OVI+BLA uncertain 15-30%

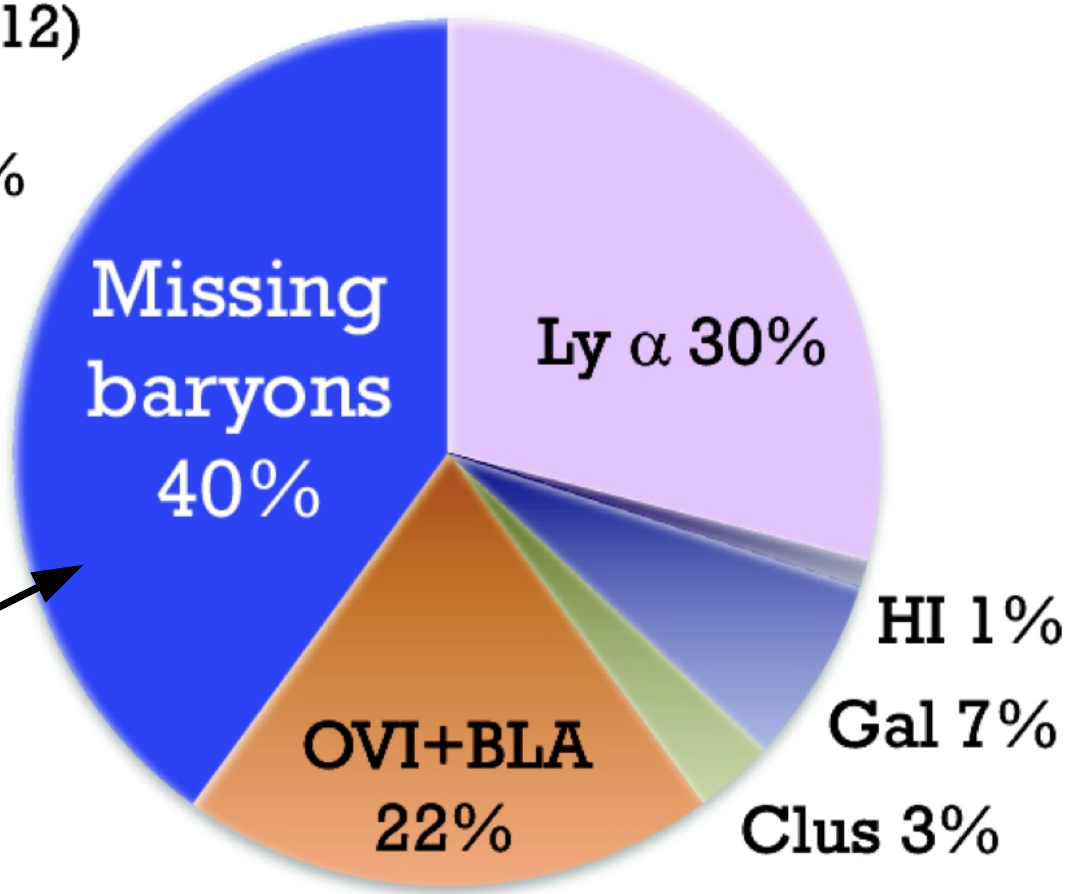

?

WHIM - warm hot intergalactic medium

Warm Hot Intergalactic Medium - Galaxy Feedback

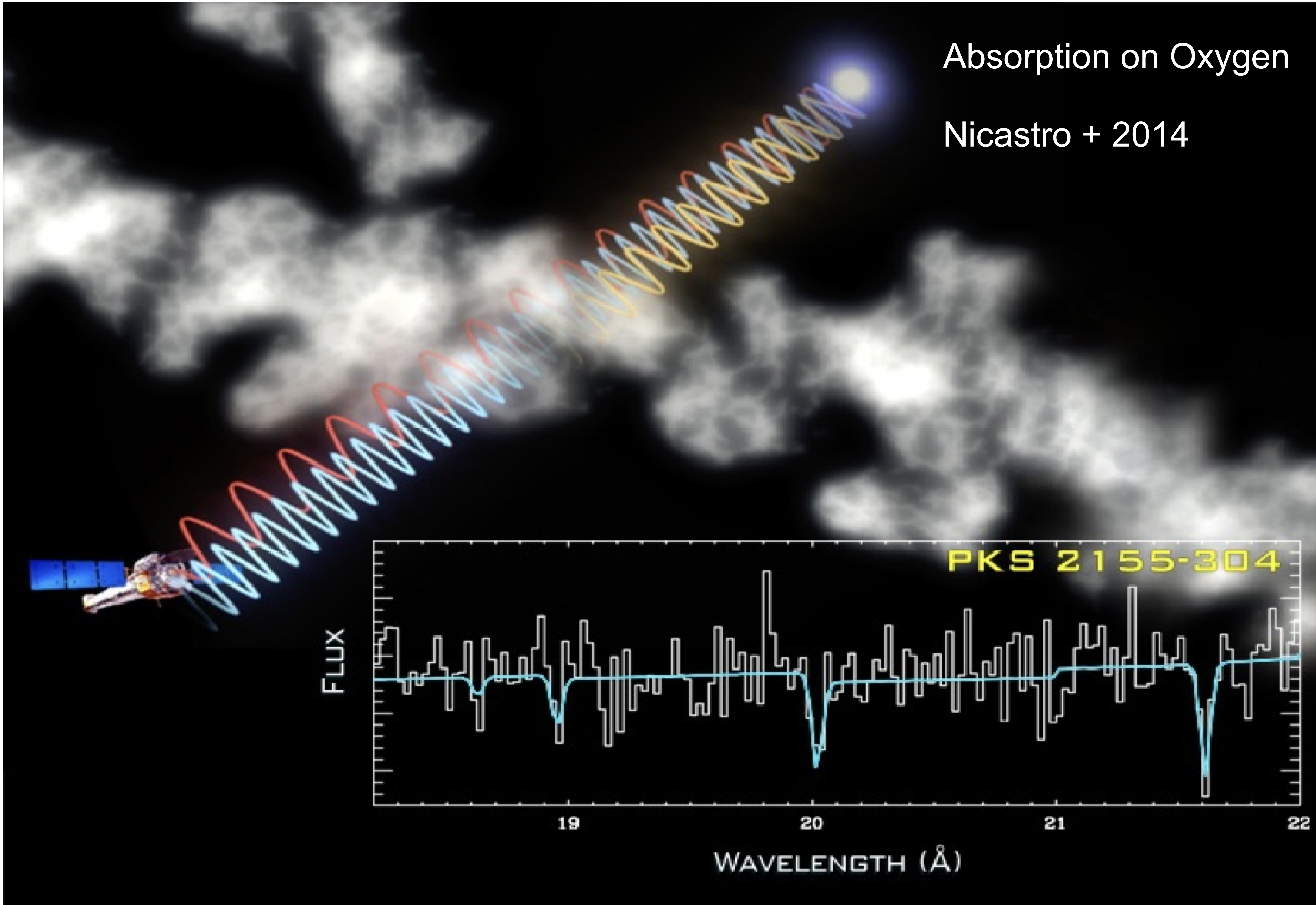

X-ray observations for Cosmology:

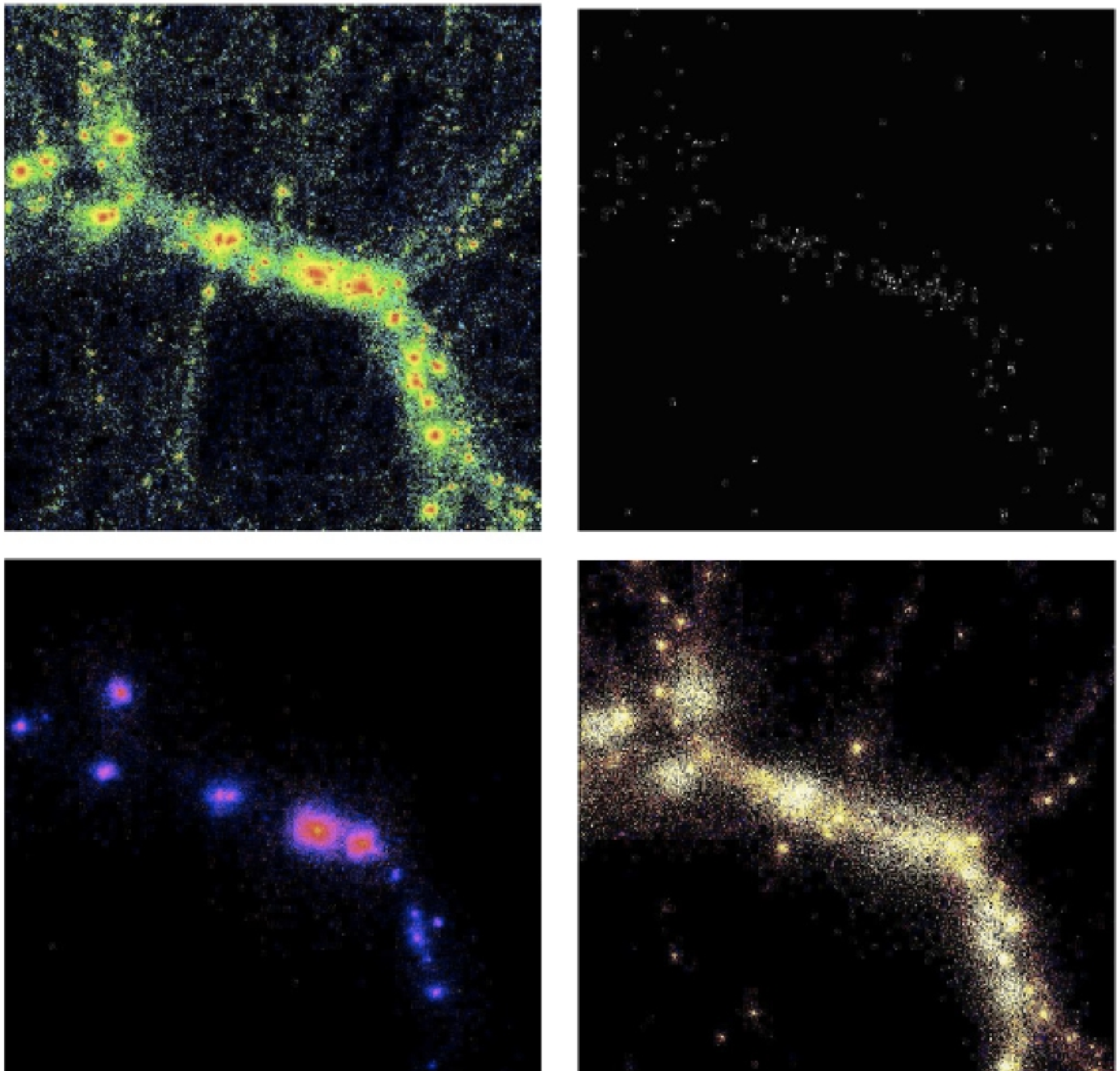

Dark Matter
26.8 %

Galaxies,
incl. Stars
$T \leqslant 10^4 K$

Clusters
$T > 10^7 K$

WHIM
$10^5 < T < 10^7 K$

Lecture on Feb. 21st – today's lecture

NEXT   NEW LECTURE   on   Feb. 23th 2023

- You can still upload your HW#6 and hands-on results
  Up to the Feb. 19th (Copernicus birthday).
- Overview of this HW#6 will be on Feb. 23rd

- theory, but we still practice

wi-fi password: a w sercu maj
We have eduroam as well